Archives of Computational Methods in Engineering (2023) 30:703–726
https://doi.org/10.1007/s11831-022-09813-9

REVIEW ARTICLE

Computational Methods to Mitigate the Effect of High Penetration of Renewable Energy Sources on Power System Frequency Regulation: A Comprehensive Review

Mahmoud H. El-Bahay[1] · **Mohammed E. Lotfy**[1] · **Mohamed A. El-Hameed**[1]

Received: 7 October 2021 / Accepted: 26 August 2022 / Published online: 11 September 2022

Abstract
Depletion of fossil fuel, global warming, and their environmental pollution clarify the importance of renewable energy sources (RESs). However, high penetration of RESs decreases power systems inertia, hence, the system becomes more sensitive to disturbances. This results in problems with frequency control because it increases the rate of change of frequency and may lead to load shedding or tripping of generating units. This paper aims at introducing a comprehensive survey of the effects of the increase in RESs on power system inertia and frequency. Different models of wind-driven and photovoltaic systems used for frequency control studies have been introduced. The up-to-date effective frequency regulation methods which can be used with highly RESs penetrated power systems have been revised and compared. These methods include virtual inertia-based methods depending on energy storage devices, de-loading of renewable energy sources, various inertial response techniques and demand response at load section including under frequency load shedding and electric vehicles. Extensive comparisons among these methods have been carried to guide power system designers, operators, researchers and grid codes taskforces in proper incorporation of RESs for frequency regulation of power systems.

1 Introduction

Depletion of fossil fuels and their environmental impacts have pushed the development of renewable energy sources (RESs) as valuable alternatives. RESs either have no inherent inertia such as photovoltaic (PV)sources, or their inertia is decoupled from frequency variations such as variable speed wind turbines (VSWTs) i.e., type 3 and 4 wind turbines (WTs). Therefore, increased integration of RESs in the electric power systems may lead to problems with frequency control and stability. Modern grid codes, such as the UK code [1], encourage the participation of offshore WTs which are larger than 50 MW in frequency regulation.

It is very important to continuously maintain the frequency of electrical power systems. Any frequency deviation (ΔF) from nominal value is an indication of unbalance between demand and generation. For example, if load demand is increased or an outage of any generating units occurs, the grid frequency will be decreased and vice versa [2]. When electrical power systems based on conventional synchronous generators (CSGs) are subjected to any abrupt load changes, the stored kinetic energy (KE) in the rotating rotors will tolerate these load changes until primary and secondary frequency control operates [3, 4]. Nowadays, the new trend for generating electricity is based on RESs due to the depletion problem of fossil fuel and some environmental issues such as global warming [5, 6]. Unfortunately, RESs are usually operated at maximum power point (MPP) unlike some of CSGs which usually contain spinning reserve which is used to overcome ΔF and steady state errors, which means that the frequency stability of power systems with increased penetration of RESs has become worrying [3, 7], specially, with the encountered increase in the rate of change of frequency (RoCoF). So, it is very important to develop new methods for frequency control to overcome the frequency stability problem [8].

Frequency regulation depends on the stored energy due the inertia of CSGs. Various studies have been devoted to increasing system inertia via virtual inertia sources. For example, the authors in [9] introduce and optimize controllers to enhance frequency stability of doubly-fed induction generator (DFIG) wind farm. While in [10], the authors have

✉ Mahmoud H. El-Bahay
mahhussen@zu.edu.eg

[1] Electrical Power and Machines Department, Faculty of Engineering, Zagazig University, Zagazig 44519, Egypt

discussed frequency regulation through controlling the rotor current of DFIG. In [11], the authors have demonstrated the role of using derivative controlled virtual inertia of energy storage systems (ESSs) and PV systems in enhancing frequency stability. Also, frequency control with RESs under load shedding is performed in [8]. In [12, 13], fuzzy logic controller is designed to determine the appropriate percentage of de-loading of wind farm (WF) in order to regulate system frequency. In [14], the authors studied the effect of the de-loading method of PV generation on power system frequency. Frequency regulation by centralized droop controller is performed for de-loaded permanent magnet synchronous generator (PMSG) offshore WF in [15]. Frequency control for PV system in microgrid using direct current (DC) link voltage and the de-loading method is introduced in [16].

ESSs with rapid response, high efficiency and large power density are suitable for frequency regulation of electric grids. A brief overview on ESSs is given in [17]. In [18], the authors have discussed the effect of hybrid energy storge (HES) on frequency stability of a microgrid. Enhancing frequency stability for an isolated system using an ultracapacitor is found in [19]. In [20], the authors illustrate the difference between proportional integral derivative (PID) and factional order PID (FOPID) controller on ΔF for hybrid fractional order power generation and ESSs. Frequency regulation with increased penetration of PV systems using EESs is studied in [4]. Battery energy storage (BES) for frequency control with increased penetration of wind energy is demonstrated in [5].

Frequency can be regulated through the inverters of RESs. This is achieved by adding a supplementary control signal that depends on either ΔF or RoCof. For example, frequency control for a microgrid with PV power plant using PV inverter is introduced in [21]. While smart PV inverter for frequency control of smart grids is justified in [22]. In addition to this, modern load management strategies and control techniques are tested for frequency control. For example, frequency control for a microgrid using the stored energy in electric vehicles (EVs) is studied in [23, 24]. Some researchers have discussed various algorithms and controllers, for example, frequency control of PV connected microgrids using fuzzy logic controllers [25], and frequency control for power systems with high penetration of RESs using a stochastic fractal optimizer [3]. Figure 1 summarizes the various methods discussed in literature for frequency regulation in the presence of RESs.

The importance of integration of RESs with electrical grids and their effects on frequency regulation has attracted many researchers, therefore, an extensive published work has been found in the literature.

This paper aims to introduce a comprehensive review of the effect of high penetration of RESs on frequency regulation of electrical power systems and to compare, evaluate and classify methods of mitigation. This work may be a guide for future grid codes regulation regarding the participation of RESs in frequency control.

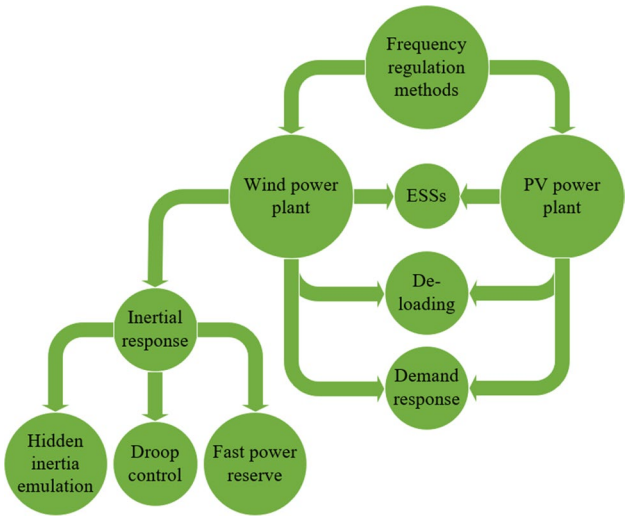

Fig. 1 Summary of the methods of frequency support with RESs

This paper is organized as follows: Sect. 2 discusses the incentives towards 100% RESs power systems and its effect on power system inertia and frequency. Modelling of RESs which include PV and wind energy is illustrated in Sect. 3. Section 4 discusses the effective frequency regulation methods for power systems with high penetration of RESs. Section 5 summarizes and concludes the paper outcomes.

2 Increased Penetration of RESs in Power Systems

Many countries around the world are now moving towards complete dependence on RESs and have set their future plans to achieve this goal. Therefore, flow of research is found in literature to study the effect of high penetration of RESs in electric grids on different aspects such as their operation and control. This section provides a summary for global rush towards replacing conventional energy sources by RESs, and a comprehensive review of their effect on power system frequency stability.

2.1 Toward Power Systems with 100% RESs

Extensive research has been done to discuss the problems of fossil fuel resources which are running out and a source of global warming [26]. The depletion of these resources is expected to occur nearly by 2050 to 2060 [27]. Emissions from these resources are mainly due to fuel burning during the electric power generation process, while emissions from renewable power plants especially wind and

solar power plants are mainly due to the fabricating process of power plant equipment (see Fig. 2) [27]. For these reasons, many conferences (like Paris agreement) have been organized to reduce these emissions and solve the problem of global warming [28]. Moreover, the climate action conference which was held in New York in 2019 by the United Nations put goals to achieve. These goals are to decrease the greenhouse emissions to 55% before 2029 and to reach zero emissions before 2050 [29]. A model which discusses the increase in fossil fuel price with depletion while using only fossil fuels and fossil fuels integrated with RESs is demonstrated in [30]. In [31], the authors investigate a method to calculate carbon dioxide emissions in Tokyo and its relation to wind speed.

Increased penetration of RESs in electric power systems will reduce both the carbon dioxide emissions and cost of electric power generation [32]. In [33], the authors discuss carbon concentration, its tax cost and vulnerability of climate change, particularly their effects on the extensive use of RESs. In [34], the authors conclude (for Egyptian grid) that the total cost reduction (fuel and environmental cost) can be 220,000$, 1,500,000$ and 2,200,000$ if the RESs are 2%, 16% and 22% of the total generation capacity respectively.

In 2016, the global electricity generations were 1096, 487, 303, 112 and 13.5 GW from hydroelectric, wind, PV, biomass and geothermal, respectively [35]. While in 2019, these values were 1310.3, 622.7, 580.16, 123.8 and 13.93 GW respectively [36]. Furthermore, it is planned for global electricity generation from RESs to reach nearly 35% before 2030 [35]. There was a significant increase in the use of RESs in the European electrical power sector from 14.3% (in 2004) to 30.8% (in 2017) [37]. Portugal is one of many countries that plan to reach 100% RESs in the electric power sector [38]. Its electric grid has a high rank in using RESs compared to other European countries, it reached 57% RESs in 2016 [39]. Also, it is expected for Kazakhstan to reach 100% RESs before 2050 [40]. A statistical for global wind and PV increased penetration is illustrated in Fig. 3 [36, 41, 42].

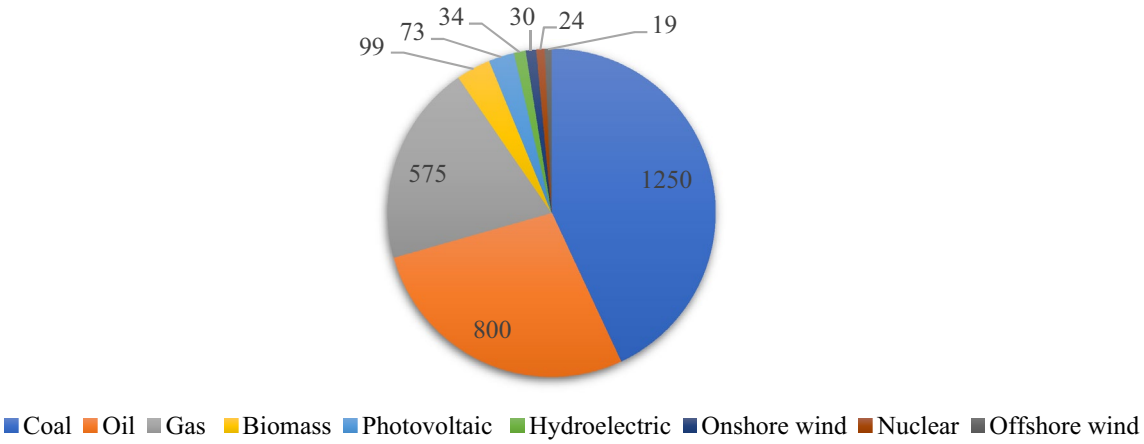

Fig. 2 Maximum carbon dioxide emissions (g/kWh) by different energy source

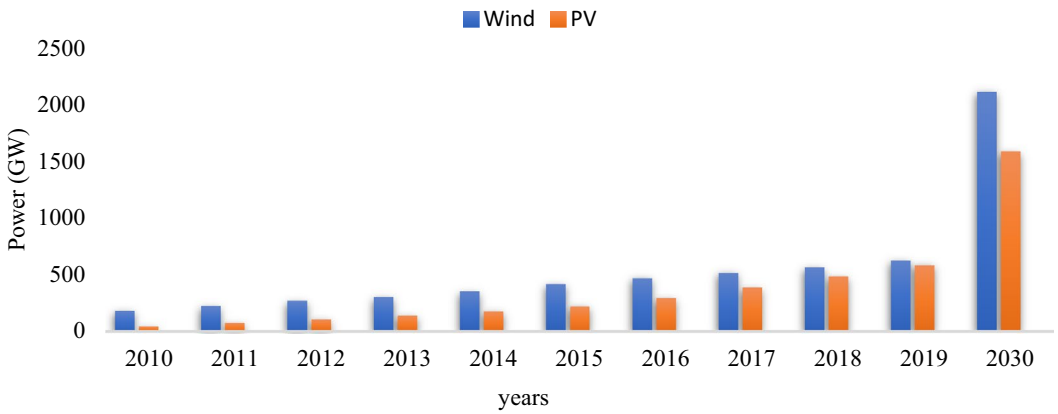

Fig. 3 Increased penetration of global wind and PV generation

2.2 Power System Inertia and Frequency Stability

Frequency stability of power systems is known as the behavior of power systems against any disturbances which tend to reduce frequency of power systems below their nominal value [43]. Inertia is known as the time duration of a generator in which the generator provides its rated power from its stored KE to the power system during disturbances as given by Eq. (1) [4, 44]. Solar PV systems do not have rotating masses, hence no stored KE, while wind generators have rotating masses but decoupled from power systems through power electronic devices and MPP techniques. So, the more the RESs penetration in power systems, the more the rated MVA of power systems with constant KE and the less the inertia of power systems as described by Eq. (2). Increasing RESs, especially solar PV and wind energy, has a negative effect on power system inertia [45]. Equation (3) shows that lower inertia power systems have faster RoCoF and higher frequency nadir (F_{nadir}) as demonstrated in Fig. 4 [6, 44]. Figure 4 describes the ΔF characteristics extracted from MATLAB/SIMULINK for a primary controlled synchronous generator with governor speed droop 5%, governor time constant 0.2 s, turbine time constant 0.5 s and is subjected to 0.1 pu power imbalance assuming zero load damping factor. Load shedding, nuisance tripping of power plants and grid blackout may occur at higher F_{nadir} and RoCoF [46, 47], which are consequences of low inertia systems.

$$H = \frac{J{\omega_n}^2}{2S_n} \tag{1}$$

$$H_{sys} = \frac{\sum KE}{S_{sys}} \tag{2}$$

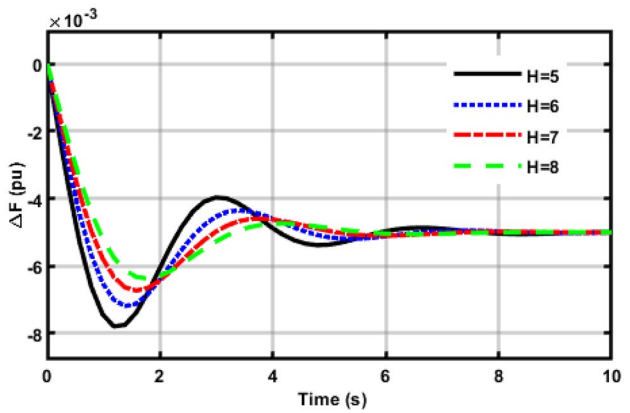

Fig. 4 Frequency deviation characteristics with different values of inertia constant

$$\frac{d\Delta f}{dt} = \frac{1}{2H_{sys}}\left(\Delta P_m - \Delta P_l - D\Delta f\right) \tag{3}$$

where H is the generator inertia, J is the generator moment of inertia, ω_n is the generator rated speed, S_n is the rated MVA of the generator, H_{sys} is the power system inertia, S_{sys} is the rated MVA of the power system, $\sum KE$ is the summation of stored KE (in MW.s) in all synchronous generators, ΔP_m is the change in generator mechanical power, ΔP_l is the change in electrical frequency independent demand and D is the load damping factor.

Many studies have been conducted to investigate how increasing RESs affects power systems. In [48, 49], the authors discuss the effect of increasing RESs on power system reliability. The authors in [50, 51], shed light on the effect of renewable distributed generators on the settings of protective devices. The effect of increased penetration of RESs on power system frequency stability is illustrated in [52–55]. While [56] discusses the effect of increasing the VSWTs and other factors on the RoCoF of the Croatian power system in case of islanding operation. Furthermore, a comparison between the frequency response of CSGs and WF is demonstrated in [57].

Therefore, the philosophy of participation of RESs in frequency has been changed. Recently, new grid codes state that RESs must participate in frequency regulation which will be discussed in detail in Sect. 4. In Germany, for example, if the power system frequency increased to 50.2 Hz, the RESs must decrease their output by a rate of 40% of their capacity per Hz [58]. On the other hand, some papers have been conducted to determine the allowable penetration level of RESs especially wind energy such as [59, 60]. The flow chart in Fig. 5 describes a criterion for calculating the acceptable level of RESs while achieving the standard F_{nadir} for the Korean power system [61]. If the minimum frequency (F_{min}) is larger than F_{nadir}, the power system can accept more RESs instead of CSGs, otherwise the limit of RESs can be calculated from the previous loop.

3 Modelling of RESs for Frequency Control

Studying the performance of power systems with high penetration of RESs requires mathematical modelling of these RESs [62]. So, the appropriate model of RESs for frequency control studies has been discussed in literature. This section discusses a literature survey into modelling of PV systems and WFs especially VSWTs.

3.1 Modeling of PV

PV systems convert solar energy into electrical energy. The efficiency of conversion is less than or equal 18%. Usually

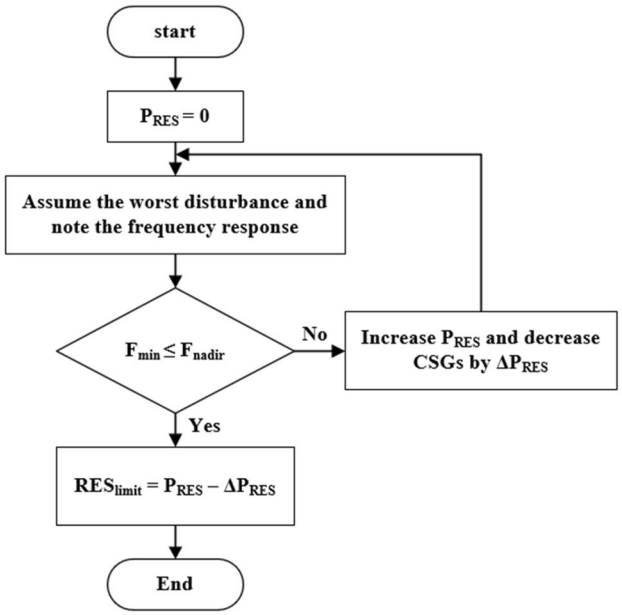

Fig. 5 Algorithm of determining the acceptable level of RESs for achieving frequency stability

bulk PV stations are equipped with maximum power point tracking (MPPT) techniques [63]. A comprehensive survey of MPPT techniques for PV is introduced in [64, 65], and PV mathematical modelling are surveyed in [66, 67]. In [68], the authors demonstrate the equivalent linearized dynamic model of a high penetration of PV energy integrated with multi-machine power system. There are different formulas in literature that describe the output power of the PV panels. These formulas are summarized in Table 1. A dynamic model of frequency droop controller of PV which is validated by [69] for PV rating larger than 10 MW is shown in Fig. 6 with the enabling of governor response, where $Freq_{ref}$ is the reference frequency, Freq is the actual frequency, P_{branch_ref} is the branch reference power, P_{branch} is the branch power, $P_{command}$ is the power command of the controller, D_{dn} is the down regulation droop, D_{up} is the up regulation droop, K_i is the integral gain of the droop controller, K_p is the proportional gain of the droop controller, T_p is the time constant of the active power filter, T_{lag} is the time constant of plant controller, Pe_{max}, Pe_{min} are the maximum and minimum power error in the droop controller respectively and P_{max}, P_{min} are the maximum and minimum power command

Table 1 Summary of various PV solar energy models

Refs	Model	Nomenclature
[82]	$P_{pv} = P_{pvstd} \times r \times \frac{I_t}{I_{std}} \times \left(1 + \beta_p \times \left(T_c - T_{std}\right)\right)$ $T_c = \frac{T_a + I_t \times \left(\frac{T_{c,rot} - T_{a,rot}}{I_{t,rot}}\right) \times \left(1 - \frac{\eta_c}{\alpha\tau} \times \left(\frac{\eta_{c,std}\left(1 - \beta_p \times T_{std}\right)}{\alpha\tau}\right)\right)}{1 + \left(T_{c,rot} - T_{a,rot}\right) \times \left(\frac{I_t}{I_{t,rot}}\right) \times \left(\frac{\beta_p \times \eta_c}{\alpha\tau}\right)}$	P_{pv} is the PV output power (KW), P_{pvstd} is the nominal power at standard condition (KW), r is the derating factor of the PV (%), I_t is the solar irradiance (KW/m^2), I_{std} is the standard condition radiation (KW/m^2), β_p is the power temperature coefficient (%/°C), T_c is the actual PV panel temperature (°C), T_{std} is the standard condition PV panel temperature (°C), T_a is the ambient temperature (°C), $T_{c,rot}$ is the rated operating temperature (°C), $T_{a,rot}$ is the ambient temperature at which $T_{c,rot}$ is calculated (°C), $I_{t,rot}$ is the solar radiation at which $T_{c,rot}$ is calculated (KW/m^2), η_c is the efficiency of electrical conversion, α is the solar absorptance, τ is the solar transmittance and $\eta_{c,std}$ is the efficiency of electrical conversion at standard conditions
[83]	$P_{PV} = \eta_{pv} \times A \times I_t$ $\eta_{pv} = \eta_{std} \times \eta_{MPPT} \times \left(1 - \beta_p \times \left(T_c - T_{std}\right)\right)$ $T_c = T_a + \left(\left(T_{c,rot} - 20\right)/800\right) \times I_t \times 1000$	A is the area of the PV panel (m^2), η_{pv} is the efficiency of the PV panel, η_{std} is the standard efficiency of the PV panel and η_{MPPT} is the efficiency of the maximum power tracking device
[84]	$P_{pv} = \frac{V_{pv} \times I_{pv} \times N_{pv}}{1000}$ $I_{pv} = I_l - I_r \times \left(e^{\left(\frac{V_{pv} + I_{pv} R_s}{a_{pv}}\right)} - 1\right) - \left(\frac{V_{pv} + I_{pv} R_s}{R_{sh}}\right)$	V_{pv} is the voltage of the PV array (V), I_{pv} is the current of the PV array (A), N_{pv} is the number of PV modules, I_l is the photogenerated current (A), I_r is the reverse saturation current of the module diode (A), R_s is the series resistance (Ω), R_{sh} is the shunt resistance (Ω) and a_{pv} is the modified ideality factor
[85]	$P_{pv} = P_{pvmax} \times I_t \times \left(1 + \beta_p \times \left(T_c - 25\right)\right) \times \eta_{conv}$ $T_c = T_a + \left(\left(T_{c,rot} - 20\right)/800\right) \times I_t \times 1000$	P_{pvmax} is the MPP of the PV at standard conditions (KW) and η_{conv} is the converter efficiency
[86]	$P_{pv} = P_{pvstd} \times I_t \times \left(1 + K_t\left(T_a + 0.0256 I_t\right) - T_{std}\right)$	K_t is a constant = -3.7×10^{-3}
[87]	$P_{pv} = \begin{cases} P_r\left(\frac{R^2}{R_c R_{std}}\right) 0 \le R < R_c \\ P_r\left(\frac{R}{R_{std}}\right) R_c \le R < R_{std} \\ P_r R_{std} \le R \end{cases}$	R is the solar irradiance factor, R_c is a certain radiation 150 W/m^2 and R_{std} is the standard radiation 1000 W/m^2
[88]	$P_{pv} = -1.69e^{-10}\left(1000 I_t\right)^4 + 1.47146e^{-7}\left(1000 I_t\right)^3$ $+2.2301e^{-5}\left(1000 I_t\right)^2 + 135.8 I_t - 0.89025$	
[89]	$P_{pv} = P_{pvstd} \times N_{pv} \times \left(\frac{I_t}{I_{std}}\right)\left(1 + \beta_p\left(T_c - T_{std}\right)\right)$	

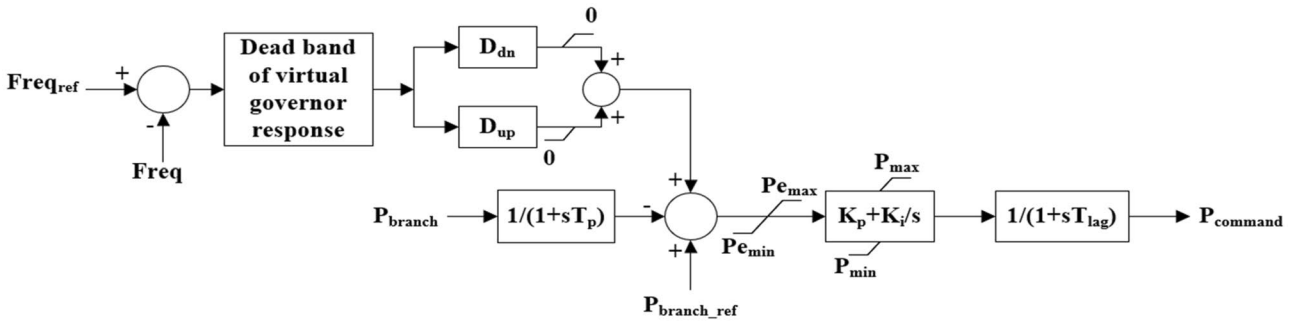

Fig. 6 Illustration of frequency control through PV active power control

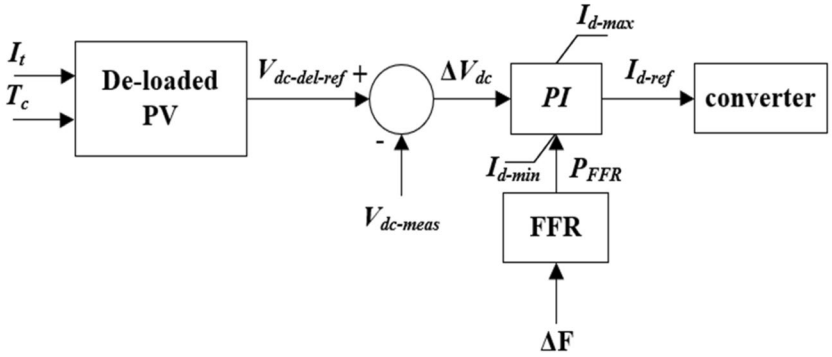

Fig. 7 Dynamic modelling of frequency regulation using de-loaded PV

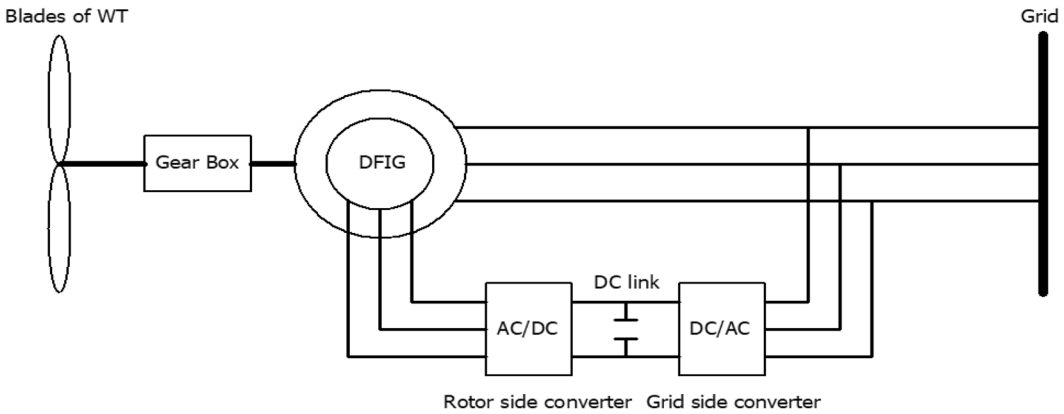

Fig. 8 Configuration diagram of type 3 WT

respectively. Also; the schematic diagram of frequency regulation using overvoltage de-loaded PV based on ΔF is shown in Fig. 7 [70], where I_t is the solar irradiance, T_c is the actual PV panel temperature, $V_{dc-del-ref}$ is the reference de-loading DC voltage, $V_{dc-meas}$ is the measured DC voltage, P_{FFR} is the fast frequency response power signal which is an emulation of droop signal of CSGs and I_{d-ref} is the reference direct axis current which control active power through PV converter.

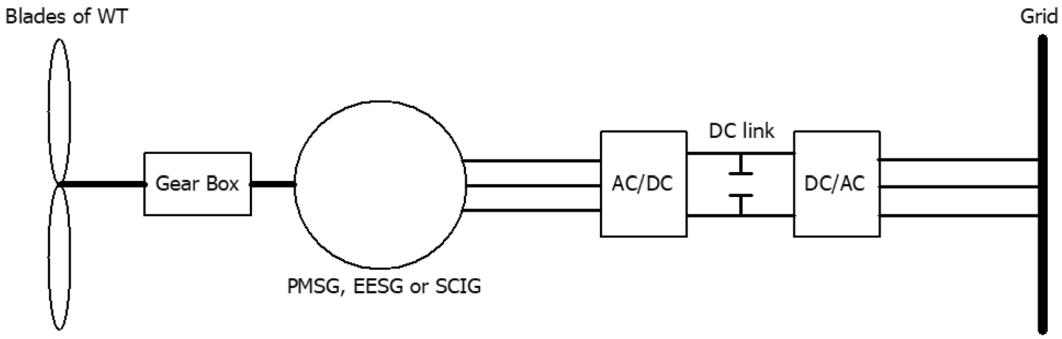

Fig. 9 Configuration diagram of type 4 WT

Table 2 Comparison between type 3 and type 4 WTs

WT type	Type 3	Type 4
Generator type	DFIG	PMSG, EESG or SCIG
% Decoupling	Partially decoupled	Fully decoupled
Configuration	See Fig. 8	See Fig. 9
Dynamic modelling	[92]	[93]

3.2 Modeling of Wind Energy

WFs can be categorized into fixed speed wind turbines (FSWTs) and VSWTs. DFIGs are the most common generators for VSWTs as they have higher efficiency than FSWTs [71, 72]. In DFIGs (type 3 WT), MPP is achieved by controlling the rotor speed through controlling rotor current by rotor side converter (RSC) [73]. A comparison between type 3 and type 4 WT is illustrated in Table 2 [74–77]. In [71], the authors discuss the various MPPT techniques for WTs.

A comprehensive survey of various modelling categories of WT generators is demonstrated in [78]. In [66, 67], a review of mathematical modeling of wind power is illustrated. The mechanical power of WT (P_{wt}) is shown by equations in Table 3. In addition to this, [79] discusses the relation between WF output power and wind speed including

Table 3 Formulas for output power of WTs

Refs	Model	Nomenclature
[57, 72]	$P_{wt} = \frac{1}{2}\rho\pi r^2 V^3 C_p$ $C_p = 0.5176\left(\frac{116}{\lambda_i} - 5 - 0.4\beta\right)e^{-\frac{21}{\lambda_i}} + 0.0068\lambda$ $\frac{1}{\lambda_i} = \frac{1}{0.08\beta+\lambda} - \frac{0.035}{\beta^3+1}$ $\lambda = \frac{\omega r}{V}$	P_{wt} is the WT output power, is ρ is the density of the air, V is the wind speed, C_p is the power coefficient, ω is the WT angular speed, r is the length of the WT blade and β is the pitch angle of the WT blade
[94]	$v = v_r\left(\frac{h}{h_r}\right)^{\gamma}$ $P_{wt} = \begin{cases} av^3 - bP_r v_{ci} < v < v_r \\ P_r v_r < v < v_{co} \\ 0 otherwise \end{cases}$ $a = \frac{P_r}{{v_r}^3 - {v_{ci}}^3}$ $b = \frac{{v_{ci}}^3}{{v_r}^3 - {v_{ci}}^3}$	h is a certain hub height,h_r is the reference height, v_r is the wind speed at h_r, v is the wind speed at h, P_r is the rated WT power, v_{ci} is the cut-in wind speed, v_{co} is the cut-out wind speed and v_r is the rated wind speed
[95]	$P_{wt} = \begin{cases} P_r\left(\frac{v^2 - {v_{ci}}^2}{{v_r}^2 - {v_{ci}}^2}\right) v_{ci} < V < v_r \\ P_r v_r < V < v_{co} \\ 0 otherwise \end{cases}$	
[67]	$P_{wt} = \frac{1}{2}\rho\pi r^2 V^3 \eta_{WG}$ $\eta_{WG} = \eta_t \eta_{gb} \eta_g$	η_t is the efficiency of WT, η_{gb} is the efficiency of the gear box and η_g is the efficiency of the generator
[88]	$P_{wt} = -2e^{-5}V^6 + 0.001V^5 - 0.0155V^4 + 0.0712V^3 + 0.1058V^2 + 0.7631V - 1.9152$	P_{wt}(kW), V (m/s)
[96]	$P_{wt} = 5.5e^{\left(\frac{V-13.8}{4.6}\right)^2} + 2.2e^{\left(\frac{V-19.15}{3.5}\right)^2}$	

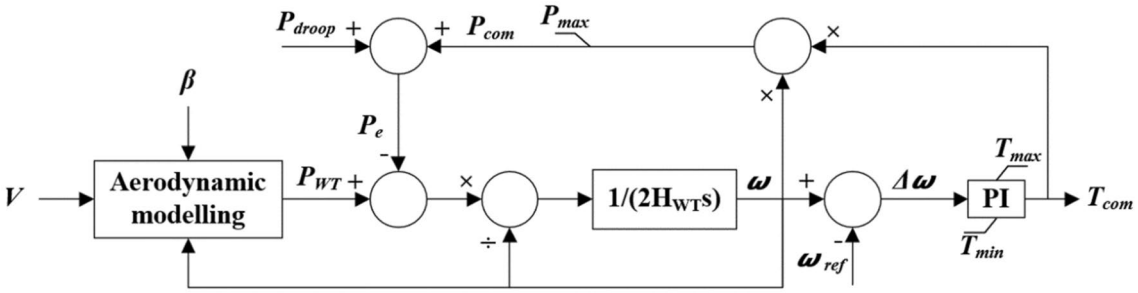

Fig. 10 Block diagram of VSWT

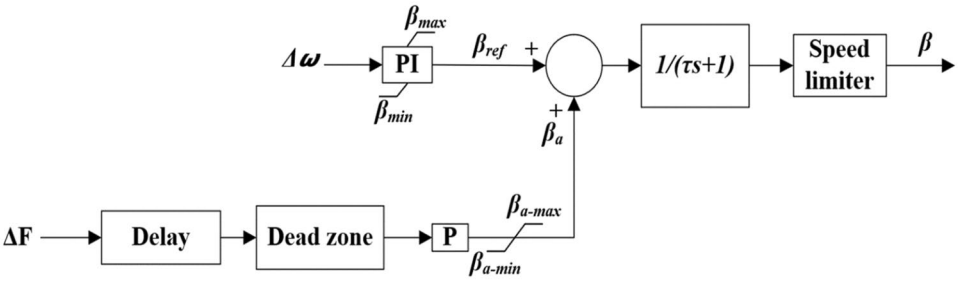

Fig. 11 Block diagram of VSWT pitch angle controller

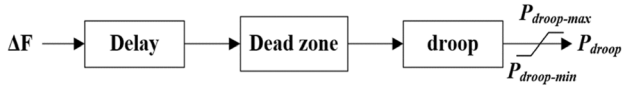

Fig. 12 Block diagram of VSWT droop controller

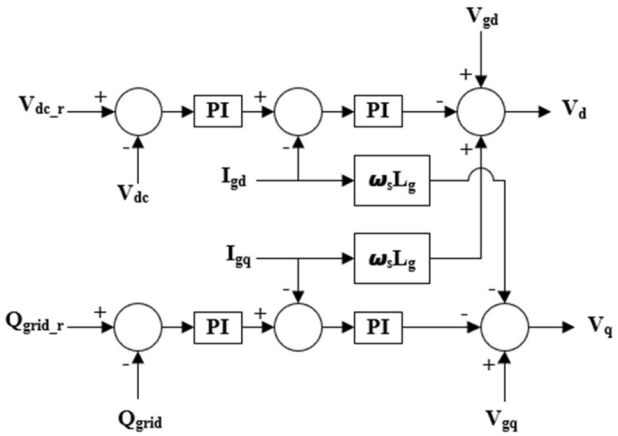

Fig. 13 Block diagram of GSC controller of type 3WT

spatial effect. While the equivalent model of single and multi-machine WF is illustrated in [72] including the model of wind speed, WT, RSC, grid side converter (GSC) and DFIG. Moreover, the equivalent model of DFIG WT is discussed in [73].The transient stability linearized model of VSWT is illustrated in [74]. In [80], the authors illustrate the transfer function (TF) of a WF which has 16 WTs. This TF relates the output active and reactive power to WF terminal voltage and wind speed. While in [81], the authors shed light on a standard model (AGC30) for RESs which is used in MATLAB/SIMULINK to study both economic dispatch and frequency regulation. The dynamic modelling of VSWT and its pitch angle and droop controllers are shown in Figs. 10, 11, 12 respectively [3], where P_e is the WT output electrical power, H_{wt} is the VSWT inertia constant, ω_{ref} is the ref VSWT speed at MPP, T_{com} is the command torque, P_{com} is the command power, β_{ref} is the pitch angle at rated rotor speed, β_a is the additional pitch angle which regulate ΔF during disturbances and τ is the time constant of the pitch angle controller.

Extensive work in literature has shed light on modelling of type 3 WT since it is the most effective and has active power regulation. Equations (4–11) describe the dynamic model of DFIG while Figs. 13 and 14 describe the modelling of rotor side controller of RSC which controls the output active and reactive power of DFIG and grid side controller of GSC which controls the voltage of the dc bus and reactive power flowing between grid and rotor respectively [72], where v_{gd},v_{gq},i_{gd},i_{gq} are d, q axis voltages and currents of the GSC respectively; v_d, v_q are d, q axis voltages of the grid respectively; i_{rd}, i_{rq} are d, q axis currents of the RSC respectively; $v_{d'}$, $v_{q'}$ are d, q axis voltages of the rotor respectively; and $\sigma = 1 - \frac{L_m^2}{L_s L_r}$.

WTs can be modeled in detail or simplified [74]. Detailed models, especially for the driven generators,

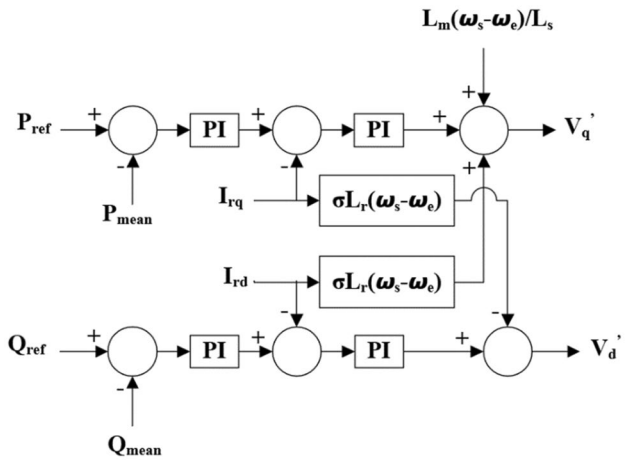

Fig. 14 Block diagram of RSC controller of type 3WT

are important to show the electromagnetic transients, however, for frequency studies simplified models can be satisfactory. For example in [73], with step variation of wind speed from 8 to 14 and back to 8 by 2 m/s steps, the results of the simplified model are accurate for both steady state and transient response (pitch angle, generator angular speed and power) with a time delay between both models less than 3% of the H constant of type 3 WT. While in [90], for wind speed 8 m/s and 0.1 pu load increasing, the results of the simplified model are accurate with small deviation in rotor speed and F_{nadir} compared with the exact model. In addition to this, the simplified model is used in [91] to test a large network which has more than 30,000 buses, 2000 SGs, a WF has 468 MW (130 × 3.6 MW WTs). The simulation results show that the simplified model is accurate for transient stability studies. From the authors' point of view, the simplified WT model is accurate, so it is recommended for frequency control studies.

$$v_{ds} = R_s i_{ds} + \frac{d\psi_{ds}}{dt} - \psi_{qs}\omega_e \tag{4}$$

$$v_{qs} = R_s i_{qs} + \frac{d\psi_{qs}}{dt} + \psi_{ds}\omega_e \tag{5}$$

$$v_{dr} = R_r i_{dr} + \frac{d\psi_{dr}}{dt} - \psi_{qr}\omega_s \tag{6}$$

$$v_{qr} = R_r i_{qr} + \frac{d\psi_{qr}}{dt} + \psi_{dr}\omega_s \tag{7}$$

$$\psi_{ds} = L_s i_{ds} + L_m i_{dr} \tag{8}$$

$$\psi_{qs} = L_s i_{qs} + L_m i_{qr} \tag{9}$$

$$\psi_{dr} = L_r i_{dr} + L_m i_{ds} \tag{10}$$

$$\psi_{qr} = L_r i_{qr} + L_m i_{qs} \tag{11}$$

where v_{ds}, v_{qs}, v_{dr}, v_{qr} are d, q axis stator and rotor voltages (V) respectively; i_{ds}, i_{qs}, i_{dr}, i_{qr} are d, q axis stator and rotor currents (KA) respectively; ψ_{ds}, ψ_{qs}, ψ_{dr}, ψ_{qr} are d, q axis stator and rotor magnetic fluxes (Wb) respectively; R_s, R_r are stator and rotor resistances (Ω) respectively; L_s, L_r are stator and rotor self inductances (mH) respectively; L_m is the mutual inductance between rotor and stator (mH), ω_e and ω_s are the rotational and slip speeds (rad/s) respectively.

4 Efficient Frequency Regulation Techniques

In this section, the common methods for frequency regulation in literature are introduced. These methods depend on adding a virtual inertia via energy storage device, deloading the RESs to have a spinning power reserve for frequency manipulation, using the load demand response for interchanging power with smart distribution networks and inertial response to support power systems with temporary active power. These.

four principles are widely discussed as follows:

4.1 Energy Storage Systems

ESSs are considered a good solution to mitigate the problem of RESs intermittency by satisfying equilibrium between load and generation while operating RESs under MPPT condition [97–99]. Their techniques can be classified as follows [97]:

- Electrical such as super capacitor energy storage (SCES) and superconducting magnetic energy storage (SMES).
- Electrochemical such as BES and fuel cell energy storage (FCES).
- Mechanical such as flywheel energy storage (FWES), pumped hydro energy storage (PHES) and compressed air energy storage (CAES).
- Chemical such as hydrogen energy storage (H_2ES).

A review of various ESSs techniques and their efficiency, life time, charging rate, discharging rate and capacity is illustrated in [100]. While [99] discusses a survey about HES mainly BES integrated with SCES. A comparison between various aspects of different ESSs techniques

Table 4 Comparison between various aspects of different types of ESSs

Type of ESSs	Fast response	High energy capacity	High efficiency	Environmental issues	High capital cost	Long lifetime
SCES	√		√		√	
SMES	√		√		√	√
CAES	√	√				
PHES		√				
FWES	√		√			√
BES	√	√	√	√	√	
FCES		√				√

is demonstrated in Table 4 [17, 101–106]. The authors in [17] shed light on various ESSs techniques which are used to smooth output power of WF. While the authors in [102] demonstrate the various control techniques which are used with BES to smooth the output power of WF. [103] illustrates the various techniques of mechanical ESSs which are used in PV and wind plants and their advantages and disadvantages. In addition to this, [107] investigates the optimal location (from power smoothing point of view) of 5 MJ SMES which integrates with renewable power systems. The authors in [108] categorize the target of ESSs into two classifications.

The power system operator must save a certain reserve active power to regulate the frequency of power systems during disturbances [104]. Using ESSs not only helps to smooth the output of RESs but also introduces frequency regulation for power systems during disturbances [109]. ESSs play an important role in regulating the frequency of power systems with high penetration of RESs as they can charge and discharge power into power systems [110]. In [111], the frequency regulation is achieved through active power control using SCES hybridized with BES for a microgrid consisting of a diesel generator and a WT. While the authors in [112] demonstrate the effect of BES location on power system frequency response due to load change at different locations. Moreover, energy control of type 3 WT integrated with FCES and SCES is illustrated in [113]. While the effect of fast response ESSs on frequency stability for Gotland island is illustrated in [114]. In addition to this, the authors in [98] investigate the effect of load increasing on frequency stability of two connected microgrids under different operating conditions of super capacitors. The authors in [115], illustrate the frequency stability of two-area power system subjected to a disturbance under three conditions. While in [116], the authors discuss the frequency regulation of a power system consisting of a diesel generator and a WT using BES under two different operating conditions. In [117], the authors investigate transient stability of an offshore WF connected to a marine current farm using a FWES based PID controller. Moreover, [118] investigates an optimization algorithm to optimize the parameters of SMES and PID which are used in secondary frequency control. A summary of some studies that have been conducted to enhance frequency stability using ESSs is given in Table 5. From the authors' point of view based on the conclusion of Tables 4 and 5, the most effective recommendation for improving the power system stability especially frequency stability is to use BES.

4.2 De-loading of RESs

As mentioned earlier, RESs operate under MPPT condition which means that they do not have any reserve power to support frequency contingency event. One method of frequency regulation techniques is to de-load RESs which means to operate below MPPT to maintain a certain reserve power for frequency regulation [14]. The de-loading of PV systems is performed by controlling the output PV voltage either by under voltage or over voltage as shown in Fig. 15 [14, 70, 123]. Over voltage de-loading is preferred due to voltage stability wise. Figure 15 is extracted from MATLAB/SIMULINK for a PV model which has a 7.34 short circuit current and a 0.6 V open circuit voltage at standard conditions. More details for de-loading of PV is given in [124].

Although de-loading of RESs below MPPT is not an efficient method for frequency regulation, it may be more effective than ESSs from cost point of view [125]. The efficient limits of PV de-loading are discussed in [125]. In [126], a cost analysis is carried out to show that the concept of de-loaded PV is economical when compared to BES for frequency control. So, many studies have been performed to illustrate frequency regulation by reserving a certain amount of active power using de-loading of RESs. Frequency regulation by active power control of PV system through inverter is investigated in [127]. [128] introduces a grid consisting of a PV system, a diesel generator and a WT and discusses the effect of using droop PV on frequency regulation while load is disturbed. While [129] discusses frequency regulation of an isolated microgrid through the de-loading of PV

Table 5 Some studies that have been performed to promote power system stability using ESSs

Refs	Technique	Type of RESs	Assumptions	Effect
[119]	SCES	PV integrated with DC microgrid	SCES is connected with BES through DC-DC converter to enhance inertia and rate of change of voltage (RoCoV)	Increasing the capacitance from 0 to 0.003 F and decreasing the virtual damping of the SCES from infinity to 1.5 will reduce the RoCoV of the DC bus voltage by 74% for 20% sudden load change
[120]	CAES	Type 3 WT	1000 MW single area power system integrated with 132 MW combustion system and 55 MW compressor	Including the CAES will reduce the ΔF by nearly 0.5 HZ
[121]	SCES	Tidal energy	Tidal power plant integrated with microgrid subjected to 0.01 pu load increasing at t = 5 s	Including the SCES will reduce the ΔF by nearly 49.4%
[114]	Inverter based ESSs	Wind energy	The wind power plant has 185 MW capacity and consisting of 75 WTG	Including ESSs will reduce the ΔF by 72.2% while the HVDC cable is faulted
[105]	FCES hybridized with FWES	Wing energy	6 MW WF consisting of 4 WTGs integrated in a microgrid which has 200 KW FWES and 200 KW FCES	The proposed system will reduce the ΔF by 0.5 HZ
[98]	SCES	PV	Two microgrids each has 100 KVA of PV power and the load disturbance is 100 KW	The proposed system will reduce the ΔF by 0.2 HZ and the contribution from the microgrid which has the disturbance is larger
[122]	SMES	Wind energy	The study is performed on Egypt power system assuming 100% of system inertia and interconnection of industrial load as a disturbance	Conventional SMES nearly reduce the ΔF by 0.15 HZ while optimal PID SMES nearly reduce ΔF by 0.2 HZ
[106]	SMES	Type 3 WT	8 type 3 WT (total capacity 200 KVA) connected to 2 diesel SGs (total capacity 800 KVA), connected to 260 KW load with a load disturbance 26 KW while the SMES is 16 KVA	The presence of SMES will reduce the ΔF to 67.04%
[117]	FWES	Wind and marine energy	80 MW offshore type 3 WT connected with 40 MW marine current farm based SCIG while the FWES is 32 MW	The presence of FES will reduce the total power fluctuation nearly by 5% under fluctuation of wind speed
[115]	BES	Wind and PV	Two-area power system has PV rating 0:880 MW and WT rating 90:880 MW	This study shows that the optimal rating of BESs is 400 MW which will reduce the maximum ΔF by 0.239 HZ
[116]	BES	Wind	300 KVA diesel SG integrated with 275 KW induction generator (WT) while BESs is 150 KW	The presence of BES will reduce the ΔF by 0.005 pu

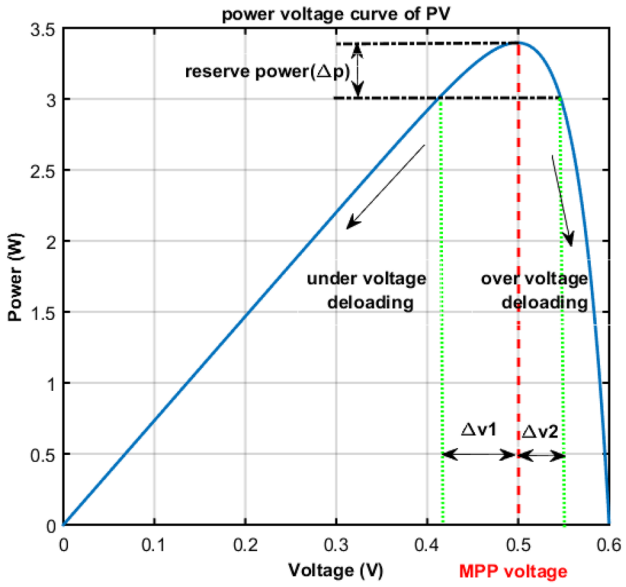

Fig. 15 Demonstrates the de-loading of PV system by under voltage and over voltage

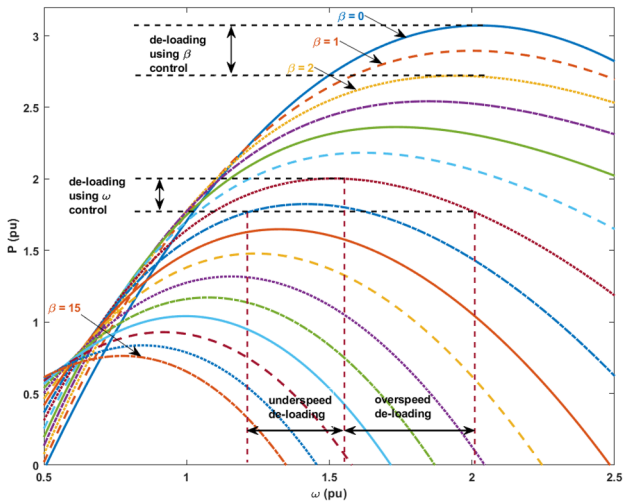

Fig. 16 Demonstration of de-loading of VSWTs by pitch angle and rotor speed control

system, the percentage of de-loading is related to the ΔF by a boost converter. Moreover, in [123] a microgrid that has 2688 KW of PV is simulated for frequency response due to 5% of load change while operating at MPP and de-loaded mode. The frequency response of northern Chile isolated grid is investigated in [70] for various PV levels and at different de-loading conditions which are MPP, 3% de-loading and 5% de-loading of PV. The results show that the level of PV slightly affects the frequency response unless the level is greater than 20% of the grid capacity. The authors in [126] combine the ΔF with the MPP voltage in the de-loading criteria of PV. For the previous case study, the authors conclude that the de-loading is more cost-effective than ESSs.

On the other hand, WTs can be de-loaded through pitch angle control or rotor speed control (over speed or under speed), over speed control is recommended due to WT frequency stability issue at under speed operation [130–132]. Pitch angle control can be performed by operating the WT at a pitch angle close to the optimal value to reserve a certain amount of power to participate in frequency regulation [130]. [133] sheds light on the de-loading of VSWTs in order to satisfy power balance and then frequency regulation. The authors in [132] shed light on the acceptable range of rotor over speed de-loading and pitch angle de-loading based on wind speed. Figure 16 illustrates the de-loading technique of VSWTs by pitch angle control and rotor speed control [12, 130, 132]. Figure 16 is extracted from MATLAB for General Electric (GE) DIFG 3.6 MW with wind speed 16 m/s. More details are given in [134–136] for frequency regulation by de-loading of VSWTs either by rotor speed control or pitch angle control.

The authors in [12] discuss the frequency regulation of a two-area power system penetrated with wind energy using de-loading technique based on adaptive PID controller. In addition to this, the authors in [137] compare the frequency response at various load disturbances while operating type 4 WT under MPPT condition and de-loading condition. While the authors in [138] compare the frequency regulation obtained from de-loading of WT while using fixed droop and wind speed adaptive droop. Moreover, the authors in [139, 140] investigate the frequency regulation introduced by traditional PID controller and adaptive PID controller which is based on artificial bee colony (ABC) algorithm. Also, the contribution of FOFPID de-loaded tidal plant on frequency regulation is discussed in [141] and compared with fixed droop, PID droop and fuzzy PID droop. Table 6 discusses the effect of de-loading of RESs on the frequency response of power systems. Based on the conclusion of various studies that have been done to improve the power system frequency, the authors prefer and recommend using ESSs rather than de-loading RESs from frequency improvement point of view although de-loading is more cost-effective than ESSs.

4.3 Demand Response

Demand response is considered an effective frequency regulation solution at the load side which can be performed by under frequency load shedding (UFLS) or by the contribution of EVs [143]. UFLS is a process of removing a certain amount of power system load when an outage of large generating unit occurs. It is performed to keep balance between generated and demand power [8]. It is performed as a last

Table 6 Summarizes the effect of the de-loading operation of RESs

Refs	Type of de-loading	Assumption	Effect
[14]	Over voltage based on adapted droop controller	The overall PV capacity is 500 KW and the PV is de-loaded by 10%	When the grid frequency is reduced from 50 to 49.9 HZ, the proposed controller increases P_{pv} by 7.6 KW. On the other hand, when the frequency is increased from 50 to 50.04 HZ P_{pv} is decreased by 3 KW
[12]	Pitch angle and over speeding the rotor of DFIG	The capacity of CSGs is 2119 MW, the capacity of wind energy is 700 MW, total load is 2734 MW with load disturbance 150 MW	Including fixed droop controller will reduce the ΔF nearly by 0.03 HZ comparing without droop controller
[142]	Over voltage based on traditional droop characteristics	The capacity of CSGs is 1800 MW, total load is 1390 MW, the capacity of PV is 100 MW with reserve power 43 MW assuming the outage of 300 MW CSG	The F_{nadir} is 48 HZ when the PV operated at MPP while the F_{nadir} is 49.2 HZ in de-loading operation
[132]	Over speed and pitch angle	The capacity of CSGs is 2650 MW, the capacity of wind energy is 500 MW, total load is 2567 MW with a sudden load disturbance 100 MW	For 7 m/s wind speed and 5% de-loading the reduction in ΔF is nearly 0.05 HZ while the reduction is nearly 0.1 HZ for 11 m/s wind speed and 10% de-loading. The more de-loading %, the more reduction in ΔF
[137]	Over speed and pitch angle	The capacity of CSGs is 2 MW, the capacity of wind energy is 2 MW with a sudden load disturbance 0.4 MW	For 8 m/s wind speed and 11.9% de-loading the reduction in ΔF is nearly 0.6 HZ while the reduction is nearly 0.3 HZ at 12 m/s wind speed and 3.5% de-loading
[138]	Over speed and pitch angle	The capacity of CSGs is 5 MW, the capacity of wind energy is 6 MW, total load is 6 MW with a sudden load disturbance 0.5 MW	The effect of using variable droop in de-loading operation will reduce the ΔF nearly by 0.05 HZ compared with fixed droop
[123]	Over voltage	The capacity of CSGs is 28 MW, the capacity of PV is 2.688 MW, total load is 30 MW, PV reserve power is 0.65 MW assuming sudden load change by 650 KW	The proposed de-loading method will reduce the ΔF by 0.321 HZ compared to MPPT operation

solution if the power system reserve power is not sufficient for power balancing [8, 143, 144].

The authors in [144] introduce a criterion for UFLS for power systems which are penetrated with high RESs and integrated with ESSs. While the effect of UFLS on New England 39 bus frequency is illustrated in [145]. Moreover, in [146] the authors discuss UFLS for a two-area power system which has 500 MW of wind energy while considering the effect of inertial control of WT. In [144] the authors discuss the effect of UFLS on the frequency response of El Hierro power system while losing the largest generating unit and also discuss the contribution of VSWT in regulating the frequency as an alternative for UFLS. In addition to this, a criterion of UFLS is performed in [147] which depends on load flow and the convergence in errors, voltage violation and frequency violation. Also, this criterion is tested by Monte Carlo simulation.

The parameters of UFLS relay depend on the system ΔF and RoCoF [143]. The role of datacenter in the optimization process of UFLS relay is illustrated in [148]. While the authors in [149] discuss the frequency response of a smart grid while using an adaptive UFLS relay which adapts its parameters each hour of the day.

Spread of EVs contributes to minimizing greenhouse gas emissions [150]. So, many researchers shed light on the impact of EVs. In [151], the authors discuss the effect of EVs on the emissions of carbon dioxide while integrating power systems with and without RESs. While [150] discusses the smart infrastructure which is required for smart EVs. In addition to this, a comprehensive detail about EVs, their ESSs and their energy consumption is discussed in [152]. Moreover, different EVs topologies with RESs based power systems are introduced in [153]. While various construction types of EVs are introduced in [154]. In addition to this, IEEE 33 bus system is studied in [155] as a case study to investigate the reduction in the cost of the system and minimizing the degradation of batteries while using EVs with RESs. Moreover, the authors in [156] optimize the integration of plug in EVs (PEVs) and RESs into power systems and verify the results on IEEE 9 bus power system.

EVs play an important role in frequency stability while minimizing UFLS at the same time [157]. [158] sheds light on the benefits of using both PV and EVs from power system stability and quality point of view. Modes of EVs which participate in frequency regulation can be classified to vehicle to grid (V2G), grid to vehicle (G2V) and EV aggregator [158]. Controlling the charging and discharging processes of EVs which are operated in G2V and V2G mode can participate in the frequency regulation of power systems while ensuring satisfaction for EV owner [158–161]. A comprehensive survey into V2G mode of EVs with RESs based power systems is introduced in [154]. V2G mode is more effective than plug in mode from frequency regulation point of view, but less effective than plug in mode from battery life time point of view [162]. EV aggregator is the communication ring between EV and power system operator which manages the charging process of EV and contributes to frequency regulation [163]. A Chinese two-area power system penetrated with wind energy is studied in [160] and discussed with the effect V2G EVs. While [164] discusses the effect of PEVs on the load frequency control (LFC) of a thermal power system based on two degrees of freedom PID. Moreover, a control methodology of EVs contribution in frequency regulation based on frequency disturbance and state of charge (SoC) is discussed in [165]. The authors in [166] illustrate a comprehensive survey about the different methods of EV charging and the effect of V2G from power system cost point of view. Usually, the droop charging control of EVs (only charging) is preferred as the discharging of EVs reduces battery life time [24]. So, the new trend of EVs is to use a secondary battery for frequency regulation [167].

The contribution of EVs in the primary frequency control of a power system integrated with RESs consisting of 38 generating units is studied in [168]. While the authors in [169] discuss intelligent energy management system for vehicle-to-vehicle (V2V) mode which is used to calculate the optimal energy supplied to grid to participate in frequency regulation. Moreover, the effect of EVs on the frequency regulation of Egyptian power system is illustrated in [170] at different levels of RESs and various load disturbances. In addition to this, [171] discusses the contribution of 1000 PEVs as an ESS for the frequency regulation of a PV grid. From the authors' point of view, EVs are more effective than UFLS based on the summarization which is given in Table 7.

4.4 Inertial Response

Inertial response is to temporarily support power systems with a certain amount of active power extracted from VSWTs based on the stored KE in the rotating masses of rotor and blades of WT. Inertia response is categorized into droop control, synthetic inertia and fast power reserve.

Droop control is an emulation of the CSGs' governor which provides additional active power during frequency disturbance according to Eq. (12) [4, 57], where ΔP is the additional active power released through the WT inverter, R_{wt} is the droop coefficient of WT. However, the fixed droop gain is not feasible due to the intermittence of wind energy. So, [172] introduces a dynamic droop controller which control the RSC controller of type 3 WT.

Synthetic inertia is an emulation of the inertial response of CSGs (fast primary response) which is used with VSWTs to extract KE during frequency disturbances [173]. The reference power signal of synthetic inertia in [173] depends

Table 7 Summarizes the effect of demand response

Refs	Demand response	Assumption	Effect
[145]	UFLS	Outage of Generator at bus 32 in New England 39 bus power system	UFLS which shed 6.088 pu will stabilize the frequency at 59.85 HZ while frequency and voltage stability unified (FVSU) which shed 2.6767 pu will stabilize the frequency at 59 HZ The more % of load shedding the less ΔF and the less economical system
[146]	UFLS	Two-area power system has 500 MW wind energy assuming 0.5 pu sudden load increasing	UFLS will shed 75% of the total mismatch power so the F_{nadir} is nearly 48.7 HZ for area1 and 48.1 HZ for area2. While fuzzy UFLS will shed 83% so the F_{nadir} is nearly 48.8 HZ for area1 and 48.2 HZ for area2. The authors notice that ΔF is slightly affected but the frequency is recovered faster in case of fuzzy UFLS
[144]	UFLS	IEEE 37 bus power system, the authors study the effect of UFLS over 24 h a day which provided in a load curve	The minimum frequency over 24 h is nearly 58.6 HZ without UFLS. While using under voltage load shedding (UVLS) and UFLS will limit the minimum frequency to 59.5 HZ
[161]	EVs	This study is performed for single and two-area power system. The capacity of single area is 10000 MVA with 15,000 EVs while the capacity of two-area is 5000 and 4000 MVA with 15,000 and 12,000 EVs respectively	For 0.2 pu load increasing in single area system the ΔF is 0.03 pu without EVs and 0.003 pu with EVs. While 0.2 pu load increasing in area1 for two-area power system will result ΔF equal 0.023 pu and 0.007 pu for area1 and area2 respectively without EVs and 0.003 pu and 0.001 pu with EVs
[165]	EVs	This study is performed on the reduced Great Britain 36 bus transmission system assuming an outage of 1724 MW generating unit	The frequency response contribution of EVs is 650 MW which will increase the minimum frequency from 49.1 to 49.57 HZ
[24]	EVs	This study is performed on an isolated microgrid which contain 2 MVA SG, 2 MVA WT and EVs with 3 KW charging power, assuming the frequency fluctuations is produced due to variation of wind speed	ΔF is 0.57 HZ at 0% of EVs, 0.5 HZ at 10% of EVs and 0.39 HZ at 30% of EVs assuming conventional droop control. The more penetration of EVs the more regulation of power system frequency
[170]	EVs	Isolated micro grid has 15 MW of CSGs, 8.5 MW of wind energy, 7.5 MW of PV, peak load 15 MW and 4.5 MWh of EVs assuming sudden load increasing by 0.1 pu	ΔF is 0.49 HZ without the effect of EVs and 0.21 HZ with the effect of virtual inertia of EVs

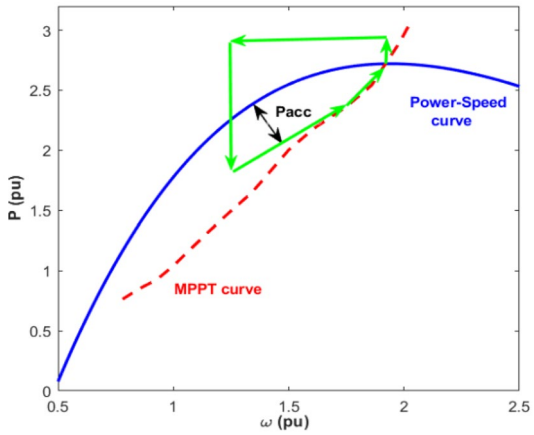

Fig. 17 Illustration of fast power reserve inertia response criterion

only on RoCoF, so the frequency could not be recovered to its nominal value. While the signal in [174] depends both on RoCoF and ΔF, so the frequency could be recovered to its nominal value.

Fast power reserve is to support the power systems with an additional KE from VSWTs by the overproduction of WT for a certain period [57]. The amount of temporary active power may reach 20% of the VSWT rating for 10 s or more [175]. The rotational speed of WT is reduced due to the overproduction process, so this KE is recovered back to the WT after the frequency disturbance is mitigated to sustain the stability of WT [57] as shown in Fig. 17. One of the fast power reserve challenges is that a secondary frequency dip (SFD) may occur during the recovering period. The SFD can be avoided through increasing the recovery period by controlling the accelerating power (P_{acc}) [57]. SFD can also be avoided by adding an additional torque signal which depends on the deviation between WT rotating speed at the beginning and at the end of the overproduction period [176]. Table 8 provides a summarization of various inertial response techniques that have been conducted to enhance the power system frequency stability.

$$\Delta P = -\frac{\Delta F}{R_{wt}} \tag{12}$$

4.5 Application of Metaheuristic Optimization on Frequency Control

Metaheuristic optimization algorithms differ from each other according to their constraints [50]. A summarization of some studies that have been conducted to enhance power system frequency based on various optimization algorithms for different frequency regulation techniques is given in Table 9.

Table 8 Enhancing the power system frequency using various inertial response techniques

Refs	Inertial response	Assumption	Effect
[177]	Fast power reserve	A grid of 20 and 80 MW SGs, 120 MW load and 16.5 MW of DFIGs (6 × 2.75 MW). Assuming the outage of 2 MW SG	The frequency nadir is 49.37 HZ without fast power reserve controller and 49.42 HZ with fast power reserve controller
[178]	Fast power reserve	A grid of 16.7 MW load, 5 MW CSG, 11.7 MW DFIGs subjected to 1.6 MW load outage	ΔF is 0.435 HZ in the MPP operation scenario of DFIGs and 0.23 HZ in the fast power reserve scenario
[179]	Droop control	The studied 150 GW power system has high penetration of WTs (50%), and 3 GW loss of generation is assumed with two scenarios. The 1st is 25% of gas turbine, in this scenario the droop gain is 0.3 MW/HZ. While the 2nd scenario is 25% of steam turbine, in this scenario the droop gain is increased to 1.05 MW/HZ due to higher response of steam turbine	The reduction in ΔF is nearly 0.07 HZ, 0.17 HZ for 1st and 2nd scenario respectively
[180]	Hidden inertia	Two-area power system, area1 has two CSGs of 380 MW, 700 MW load and 500 MW WF while area2 has two CSGs of 380 MW and 800 MW load. Assuming 8 m/s wind speed and 0.05 pu sudden load increasing in area1	ΔF is reduced by 0.04 HZ during hidden inertia emulation
[181]	Hidden inertia	The studied system consists of two CSGs 1000 MW and 400 MW, 1300 MW load and 600 MW DFIG. Assuming 7 m/s wind speed and 50 MW sudden load increasing	ΔF is 0.24 HZ, 0.19 HZ and 0.16 HZ for no inertia response, one loop synthetic inertia and two loop synthetic inertia respectively

Table 9 Promoting power system frequency stability based on optimization algorithms

Refs	Frequency regulation	Optimization algorithm	Optimized problem	Effect	Conclusion
[182]	BES hybridized with FWES	Firefly (FF) hybridized with particle swarm (PSO)	Optimal parameters of PID controller	With the PSO-PID the ΔF is nearly 0.003 pu, FF-PID reduce ΔF nearly to 0.001 pu while FF-PSO-PID reduce ΔF nearly to 0.0005 pu	Integrating of FF and PSO provides more efficient performance and integral absolute error than FF and PSO for the studied system
[183]	SCES	Sine cosine algorithm (SCA) compared with PSO	Optimal parameters of PI controller	For 0.01 pu sudden load increasing in area1 of two-area power system based on poolco contraction the ΔF nearly is 0.01 HZ for both SCA and PSO but SCA is faster and less oscillation response than PSO	SCA is more efficient than PSO for the studied system from the speed of performance point of view
[3]	Extracting of KE from WT, BES for PV	Stochastic fractal optimizer (SFO)	Optimal setting of frequency regulation controllers	For 0.05 pu sudden load increasing in area2 the ΔF of area1 and area2 is 0.0042 pu, 0.0083 pu for conventional PID and 0.0013 pu, 0.0035pu for SFO-PID respectively	For the studied two are power system based on either MPP operation of WT or virtual inertia, SFO algorithm is more efficient than genetic algorithm (GA)
[184]	SMES and BES	Social spider optimizer (SSO)	Optimal setting of PID controller	Based on SSO the ΔF is 0.0014 pu, 0.0082 pu for area1 and area2 respectively for 0.05 pu sudden load increasing in area1	SSO is a robust and fast algorithm for RESs fluctuations and sudden load disturbances
[185]	EVs	Genetic algorithm optimizer (GAO)	Optimal setting of fuzzy PI controller for optimal charging and discharging of EVs	For multi-step load change in the studied power system including RESs, EVs and CSGs while using GA-FPI the first ΔF is nearly reduced by 0.05 pu comparing to PI	GA-FPI is more efficient than PI for the four studied cases of the isolated microgrid

5 Conclusion

This paper discussed the motivative issues towards the 100% use of RESs power systems and its effect on power system inertia, ΔF and RoCoF. Moreover, the dynamic modelling of PV and various WTs especially type 3 and 4 and their controllers which are used for frequency stability study were illustrated in this paper. Also, various frequency regulation methods, their advantages and disadvantages were discussed. In addition to this, some metaheuristic optimization algorithms were illustrated. Comprehensive comparisons between various frequency regulation methods have been made in this paper to help researchers and grid operators to select the most effective method to optimize the ΔF and RoCoF. From the authors' point of view based on various papers conclusion, ESSs especially BES are more effective than the de-loading of renewable energy sources from frequency regulation point of view. The authors recommend resorting the de-loading of renewable energy sources at very high penetrations while the spinning reserve of CSGs is not sufficient to support power system frequency disturbances. Demand response is considered a good solution to regulate frequency, but it requires an excellent communication infrastructure between generation and demand sectors. Various demand response techniques which are UFLS and EVs including their advantages and disadvantages were introduced in this paper. Inertia response is an excellent, cost-effective and fast frequency regulation solution and the most spreading technique, but it may cause a SFD during the power recovery period as it is a temporary technique. Prolongation of the recovery time can avoid the problem of SFD. For further studies, the authors recommend studying the effect of the prolongation of the recovery time on a wider scale and the effect of various electric vehicle topologies on frequency stability.

Funding Open access funding provided by The Science, Technology & Innovation Funding Authority (STDF) in cooperation with The Egyptian Knowledge Bank (EKB).

Data Availability Not applicable.

Declarations

Conflict of interest The authors declare no conflict of interest.

Ethical Approval The study did not involve humans or animals.

Informed Consent The study did not involve humans.

References

1. Robles E, Haro-Larrode M, Santos-Mugica M, Etxegarai A, Tedeschi E (2019) Comparative analysis of European grid codes relevant to offshore renewable energy installations. Renew Sustain Energy Rev 102:171–185. https://doi.org/10.1016/j.rser.2018.12.002
2. Tang ZX, Lim YS, Morris S, Yi JL, Lyons PF, Taylor PC (2019) A comprehensive work package for energy storage systems as a means of frequency regulation with increased penetration of photovoltaic systems. Int J Electr Power Energy Syst 110:197–207. https://doi.org/10.1016/j.ijepes.2019.03.002
3. El-Hameed MA, Elkholy MM, El-Fergany AA (2019) Efficient frequency regulation in highly penetrated power systems by renewable energy sources using stochastic fractal optimiser. IET Renew Power Gener 13(12):2174–2183. https://doi.org/10.1049/iet-rpg.2019.0186
4. Fernández-Guillamón A, Gómez-Lázaro E, Muljadi E, Molina-García Á (2019) Power systems with high renewable energy sources: A review of inertia and frequency control strategies over time. Renew Sustain Energy Rev 115:109369. https://doi.org/10.1016/j.rser.2019.109369
5. Datta U, Kalam A, Shi J (2019) The relevance of large-scale battery energy storage (BES) application in providing primary frequency control with increased wind energy penetration. J Energy Storage 23:9–18. https://doi.org/10.1016/j.est.2019.02.013
6. Karbouj H, Rather ZH, Flynn D, Qazi HW (2019) Non-synchronous fast frequency reserves in renewable energy integrated power systems: A critical review. Int J Electr Power Energy Syst 106:488–501. https://doi.org/10.1016/j.ijepes.2018.09.046
7. Fini MH, Golshan MEH (2019) Frequency control using loads and generators capacity in power systems with a high penetration of renewables. Electric Power Syst Res 166:43–51. https://doi.org/10.1016/j.epsr.2018.09.010
8. Silva SS Jr, Assis TML (2020) Adaptive underfrequency load shedding in systems with renewable energy sources and storage capability. Electric Power Syst Res 189:106747. https://doi.org/10.1016/j.epsr.2020.106747
9. Liu J, Yang Z, Yu J, Huang J, Li W (2020) Coordinated control parameter setting of DFIG wind farms with virtual inertia control. Int J Electr Power Energy Syst 122:1061–1067. https://doi.org/10.1016/j.ijepes.2020.106167
10. Tian X, Wang W, Chi Y, Li Y, Liu C (2017) Adaptation virtual inertia control strategy of DFIG and assessment of equivalent virtual inertia time constant of connected power system. J Eng 2017(13):922–928. https://doi.org/10.1049/joe.2017.0464
11. Saxena P, Singh N, Pandey AK (2020) Enhancing the dynamic performance of microgrid using derivative controlled solar and energy storage based virtual inertia system. J Energy Storage 31:101613. https://doi.org/10.1016/j.est.2020.101613
12. Abazari A, Monsef H, Wu B (2019) Load frequency control by de-loaded wind farm using the optimal fuzzy-based PID droop controller. IET Renew Power Gener 13(1):180–190. https://doi.org/10.1049/iet-rpg.2018.5392

13. Pradhan C, Bhende C (2015) Enhancement in primary frequency contribution using dynamic deloading of wind turbines. IFAC-Papers Online 48(30):13–18. https://doi.org/10.1016/j.ifacol.2015.12.346
14. Yan G, Liang S, Jia Q, Cai Y (2019) Novel adapted de-loading control strategy for PV generation participating in grid frequency regulation. J Eng 2019(16):3383–3387. https://doi.org/10.1049/joe.2018.8481
15. Jahan E, Hazari MR, Muyeen S, Umemura A, Takahashi R, Tamura J (2019) Primary frequency regulation of the hybrid power system by deloaded PMSG-based offshore wind farm using centralised droop controller. J Eng 2019(18):4950–4954. https://doi.org/10.1049/joe.2018.9326
16. Lyu X, Xu Z, Zhao J (2018) A coordinated frequency control strategy for photovoltaic system in microgrid. J Int Council Electr Eng 8(1):37–43. https://doi.org/10.1080/22348972.2018.1470295
17. Barra P, de Carvalho W, Menezes T, Fernandes R, Coury D (2020) A review on wind power smoothing using high-power energy storage systems. Renew Sustain Energy Rev 137:110455. https://doi.org/10.1016/j.rser.2020.110455
18. Li J et al (2016) A novel use of the hybrid energy storage system for primary frequency control in a microgrid. Energy Procedia 103:82–87. https://doi.org/10.1016/j.egypro.2016.11.253
19. Delille G, Francois B, Malarange G (2012) Dynamic frequency control support by energy storage to reduce the impact of wind and solar generation on isolated power system's inertia. IEEE Trans Sustain Energy 3(4):931–939. https://doi.org/10.1109/TSTE.2012.2205025
20. Nosrati K, Mansouri HR, Saboori H (2017) Fractional-order PID controller design of frequency deviation in a hybrid renewable energy generation and storage system. CIRED-Open Access Proc J 2017(1):1148–1152. https://doi.org/10.1049/oap-cired.2017.0248
21. Hsu C-T, Cheng T-J, Huang H-M, Lee Y-D, Chang Y-R, Jiang J-L (2019) Over frequency control of photovoltaic inverters in an island microgrid. Microelectron Reliab 92:42–54. https://doi.org/10.1016/j.microrel.2018.11.011
22. Howlader AM, Sadoyama S, Roose LR, Chen Y (2020) Active power control to mitigate voltage and frequency deviations for the smart grid using smart PV inverters. Appl Energy 258:114000. https://doi.org/10.1016/j.apenergy.2019.114000
23. Li P, Hu W, Xu X, Huang Q, Liu Z, Chen Z (2019) A frequency control strategy of electric vehicles in microgrid using virtual synchronous generator control. Energy 189(116389):2019. https://doi.org/10.1016/j.energy.2019.116389
24. Zhu X, Xia M, Chiang H-D (2018) Coordinated sectional droop charging control for EV aggregator enhancing frequency stability of microgrid with high penetration of renewable energy sources. Appl Energy 210:936–943. https://doi.org/10.1016/j.apenergy.2017.07.087
25. Rajesh T, Gunapriya B, Sabarimuthu M, Karthikkumar S, Raja R, Karthik M (2020) Frequency control of PV-connected micro grid system using fuzzy logic controller. Mater Today 45:2260–2264. https://doi.org/10.1016/j.matpr.2020.10.255
26. Capellán-Pérez I, Mediavilla M, de Castro C, Carpintero Ó, Miguel LJ (2014) Fossil fuel depletion and socio-economic scenarios: An integrated approach. Energy 77:641–666. https://doi.org/10.1016/j.energy.2014.09.063
27. Shahsavari A, Yazdi FT, Yazdi HT (2019) Potential of solar energy in Iran for carbon dioxide mitigation. Int J Environ Sci Technol 16:507–524. https://doi.org/10.1007/s13762-018-1779-7
28. Lin B, Chen Y (2020) The rapid development of the photovoltaic industry in China and related carbon dioxide abatement costs. Reg Environ Change 20:49. https://doi.org/10.1007/s10113-020-01633-6
29. Mutezo G, Mulopo J (2021) A review of Africa's transition from fossil fuels to renewable energy using circular economy principles. Renew Sustain Energy Rev 137:110609. https://doi.org/10.1016/j.rser.2020.110609
30. Barreto RA (2018) Fossil fuels, alternative energy and economic growth. Econ Model 75:196–220. https://doi.org/10.1016/j.econmod.2018.06.019
31. Babenhauserheide A, Hase F, Morino I (2020) Net CO2 fossil fuel emissions of Tokyo estimated directly from measurements of the Tsukuba TCCON site and radiosondes. Atmos Meas Tech 13:2697–2710. https://doi.org/10.5194/amt-13-2697-2020
32. Sidorov D et al (2020) Toward zero-emission hybrid AC/DC power systems with renewable energy sources and storages: a case study from lake Baikal region. Energies 13(5):1226. https://doi.org/10.3390/en13051226
33. Hao F, Shao W (2021) What really drives the deployment of renewable energy? A global assessment of 118 countries. Energy Res Soc Sci 72:101880. https://doi.org/10.1016/j.erss.2020.101880
34. Nassar IA, Hossam K, Abdella MM (2019) Economic and environmental benefits of increasing the renewable energy sources in the power system. Energy Rep 5:1082–1088. https://doi.org/10.1016/j.egyr.2019.08.006
35. Adefarati T, Bansal RC (2019) Application of renewable energy resources in a microgrid power system. J Eng 2019(18):5308–5313. https://doi.org/10.1049/joe.2018.9261
36. International Renewable Energy Agency, Renewable Capacity Statistics (2020) https://irena.org/publications/2020/Mar/Renewable-Capacity-Statistics-2020; Accessed 10 March 2021
37. Loumakis S, Giannini E, Maroulis Z (2019) Renewable energy sources penetration in Greece: characteristics and seasonal variation of the electricity demand share covering. Energies 12(12):2441. https://doi.org/10.3390/en12122441
38. Yue X et al (2020) Least cost energy system pathways towards 100% renewable energy in Ireland by 2050. Energy 207:118264. https://doi.org/10.1016/j.energy.2020.118264
39. Doepfert M, Castro R (2021) Techno-economic optimization of a 100% renewable energy system in 2050 for countries with high shares of hydropower: the case of Portugal. Renewable Energy 165:491–503. https://doi.org/10.1016/j.renene.2020.11.061
40. Bogdanov D, Toktarova A, Breyer C (2019) Transition towards 100% renewable power and heat supply for energy intensive economies and severe continental climate conditions: Case for Kazakhstan. Appl Energy 253:113606. https://doi.org/10.1016/j.apenergy.2019.113606
41. Global Wind Energy Council, Wind could supply 20% of global power by 2030: GWEC, https://gwec.net/wind-could-supply-20-of-global-power-by-2030-gwec. Accessed 10 March 2021
42. Research and Markets-Market Research Reports, Solar Photovoltaic (PV) Market, Update 2019 -Global Market Size, Market Share, Average Price, Regulations, and Key Country Analysis to 2030, https://www.researchandmarkets.com/reports/4855772/solar-photovoltaic-pv-market-update-2019#src-pos-1. Accessed 10 March 2021
43. Johnson SC, Papageorgiou DJ, Mallapragada DS, Deetjen TA, Rhodes JD, Webber ME (2019) Evaluating rotational inertia as a component of grid reliability with high penetrations of variable renewable energy. Energy 180:258–271. https://doi.org/10.1016/j.energy.2019.04.216
44. Fernández-Guillamón A, Vigueras-Rodríguez A, Molina-García Á (2019) Analysis of power system inertia estimation in high wind power plant integration scenarios. IET Renew Power Gener 13(15):2807–2816. https://doi.org/10.1049/iet-rpg.2019.0220
45. Mehigan L, Al-Kez D, Collins S, Foley A, Ógallachóir B, Deane P (2020) Renewables in the European power system and the

impact on system rotational inertia. Energy 203:117776. https://doi.org/10.1016/j.energy.2020.117776
46. Al-Kez D et al (2020) A critical evaluation of grid stability and codes, energy storage and smart loads in power systems with wind generation. Energy 205:117671. https://doi.org/10.1016/j.energy.2020.117671
47. Fang J, Li H, Tang Y, Blaabjerg F (2019) On the inertia of future more-electronics power systems. IEEE J Emerging Select Top Power Electron 7(4):2130–2146. https://doi.org/10.1109/JESTPE.2018.2877766
48. Steele AJH, Burnett JW, Bergstrom JC (2021) The impact of variable renewable energy resources on power system reliability. Energy Policy 151:111947. https://doi.org/10.1016/j.enpol.2020.111947
49. Diesendorf M, Elliston B (2018) The feasibility of 100% renewable electricity systems: a response to critics. Renew Sustain Energy Rev 93:318–330. https://doi.org/10.1016/j.rser.2018.05.042
50. Draz A, Elkholy MM, El-Fergany AA (2021) Soft computing methods for attaining the protective device coordination including renewable energies: review and prospective. Archiv Computat Methods Eng. https://doi.org/10.1007/s11831-021-09534-5
51. Razavi S-E et al (2019) Impact of distributed generation on protection and voltage regulation of distribution systems: a review. Renew Sustain Energy Rev 105:157–167. https://doi.org/10.1016/j.rser.2019.01.050
52. Homan S, Dowell NM, Brown S (2021) Grid frequency volatility in future low inertia scenarios: challenges and mitigation options. Appl Energy 290:116723. https://doi.org/10.1016/j.apenergy.2021.116723
53. Mararakanye N, Bekker B (2019) Renewable energy integration impacts within the context of generator type, penetration level and grid characteristics. Renew Sustain Energy Rev 108:441–451. https://doi.org/10.1016/j.rser.2019.03.045
54. Ratnam KS, Palanisamy K, Yang G (2020) Future low-inertia power systems: Requirements, issues, and solutions: a review. Renew Sustain Energy Rev 124:109773. https://doi.org/10.1016/j.rser.2020.109773
55. Tielens P, Van Hertem D (2016) The relevance of inertia in power systems. Renew Sustain Energy Rev 55:999–1009. https://doi.org/10.1016/j.rser.2015.11.016
56. Đaković J, Krpan M, Ilak P, Baškarad T, Kuzle I (2020) Impact of wind capacity share, allocation of inertia and grid configuration on transient RoCoF: the case of the Croatian power system. Int J Electr Power Energy Syst 121:106075. https://doi.org/10.1016/j.ijepes.2020.106075
57. Cheng Y, Azizipanah-Abarghooee R, Azizi S, Ding L, Terzija V (2020) Smart frequency control in low inertia energy systems based on frequency response techniques: a review. Appl Energy 279:115798, https://doi.org/10.1016/j.apenergy.2020.115798
58. Tsili M, Papathanassiou S (2009) A review of grid code technical requirements for wind farms. IET Renew Power Gener 3(3):308–332. https://doi.org/10.1049/iet-rpg.2008.0070
59. Ulam-Orgil C, Lee H-W, Kang Y-C (2012) Evaluation of the wind power penetration limit and wind energy penetration in the Mongolian central power system. J Electr Eng Technol 7(6):852–858. https://doi.org/10.5370/JEET.2012.7.6.852
60. Yoon M, Yoon Y-T, Jang G (2015) A study on maximum wind power penetration limit in island power system considering high-voltage direct current interconnections. Energies 8(12):14244–14259. https://doi.org/10.3390/en81212425
61. Gwon HN, Choi WY, Kook KS (2019) Evaluation method for penetration limit of renewable energy sources in Korean power system. Energies 12(21):4207. https://doi.org/10.3390/en12214207
62. Nadjemi O, Nacer T, Hamidat A, Salhi H (2017) Optimal hybrid PV/wind energy system sizing: application of cuckoo search algorithm for Algerian dairy farms. Renew Sustain Energy Rev 70:1352–1365. https://doi.org/10.1016/j.rser.2016.12.038
63. Kavya M, Jayalalitha S (2020) Developments in perturb and observe algorithm for maximum power point tracking in photo voltaic panel: a review. Archiv Comput Methods Eng 28(2):2447–2457. https://doi.org/10.1007/s11831-020-09461-x
64. Khan MJ, Mathew L (2017) Different kinds of maximum power point tracking control method for photovoltaic systems: a review. Archiv Comput Methods Eng 24(4):855–867. https://doi.org/10.1007/s11831-016-9192-1
65. Khan MJ (2020) Review of recent trends in optimization techniques for hybrid renewable energy system. Archi Comput Methods Eng 28:1459–1469. https://doi.org/10.1007/s11831-020-09424-2
66. Emad D, El-Hameed M, Yousef M, El-Fergany A (2019) Computational methods for optimal planning of hybrid renewable microgrids: a comprehensive review and challenges. Archi Comput Methods Eng 27:1297–1319. https://doi.org/10.1007/s11831-019-09353-9
67. Gaabour A, Metatla A, Kelaiaia R, Bourennani F, Kerboua A (2019) Recent bibliography on the optimization of multi-source energy systems. Archi Comput Methods Eng 26(4):809–830. https://doi.org/10.1007/s11831-018-9271-6
68. Bi JT, Du W, Wang HF (2015) Aggregated dynamic model of grid-connected PV generation farms. IET Conf Proc. https://doi.org/10.1049/cp.2015.0527
69. Western Electricity Coordinating Council Modeling and Validation Work Group, Generic Solar Photovoltaic System Dynamic Simulation Model Specification, https://www.powerworld.com/files/WECC-Solar-PV-Dynamic-Model-Specification-September-2012; [accessed 18 August 2021].
70. Rahmann C, Castillo AJE (2014) Fast frequency response capability of photovoltaic power plants: the necessity of new grid requirements and definitions. Energies 7(10):6306–6322. https://doi.org/10.3390/en7106306
71. Karad S, Thakur R (2021) Recent trends of control strategies for doubly fed induction generator based wind turbine systems: a comparative review. Archi Comput Methods Eng 28(1):15–29. https://doi.org/10.1007/s11831-019-09367-3
72. Zou J, Peng C, Yan Y, Zheng H, Li Y (2014) A survey of dynamic equivalent modeling for wind farm. Renew Sustain Energy Rev 40:956–963. https://doi.org/10.1016/j.rser.2014.07.157
73. Ochoa D, Martinez S (2014) Fast-frequency response provided by DFIG-wind turbines and its impact on the grid. IEEE Trans Power Syst 32(5):4002–4011. https://doi.org/10.1109/TPWRS.2016.2636374
74. Honrubia-Escribano A, Gómez-Lázaro E, Fortmann J, Sørensen P, Martin-Martinez S (2018) Generic dynamic wind turbine models for power system stability analysis: A comprehensive review. Renew Sustain Energy Rev 81:1939–1952. https://doi.org/10.1016/j.rser.2017.06.005
75. Rahimi M, Asadi M (2019) Control and dynamic response analysis of full converter wind turbines with squirrel cage induction generators considering pitch control and drive train dynamics. Int J Electr Power Energy Syst 108:280–292. https://doi.org/10.1016/j.ijepes.2019.01.018
76. Xia SW, Bu SQ, Zhang X, Xu Y, Zhou B, Zhu JB (2018) Model reduction strategy of doubly-fed induction generator-based wind farms for power system small-signal rotor angle stability analysis. Appl Energy 222:608–620. https://doi.org/10.1016/j.apenergy.2018.04.024
77. Zong H, Lyu J, Wang X, Zhang C, Zhang R, Cai X (2021) Grey box aggregation modeling of wind farm for wideband oscillations

analysis. Appl Energy 283:116035. https://doi.org/10.1016/j.apenergy.2020.116035
78. He X, Geng H, Mu G (2021) Modeling of wind turbine generators for power system stability studies: a review. Renew Sustain Energy Rev 143:110865. https://doi.org/10.1016/j.rser.2021.110865
79. Jin Y, Ju P, Rehtanz C, Wu F, Pan X (2018) Equivalent modeling of wind energy conversion considering overall effect of pitch angle controllers in wind farm. Appl Energy 222:485–496. https://doi.org/10.1016/j.apenergy.2018.03.180
80. Wu F et al (2019) Transfer function based equivalent modeling method for wind farm. J Modern Power Syst Clean Energy 7(3):549–557. https://doi.org/10.1007/s40565-018-0410-8
81. Jie B, Tsuji T, Uchida K (2017) Analysis and modelling regarding frequency regulation of power systems and power supply–demand-control based on penetration of renewable energy sources. J Eng 2017(13):1824–1828. https://doi.org/10.1049/joe.2017.0646
82. Baruah A, Basu M, Amuley D (2021) Modeling of an autonomous hybrid renewable energy system for electrification of a township: A case study for Sikkim India. Renew Sustain Energy Rev 135:110158. https://doi.org/10.1016/j.rser.2020.110158
83. Lan H, Wen S, Hong Y-Y, David CY, Zhang L (2015) Optimal sizing of hybrid PV/diesel/battery in ship power system. Appl Energy 158:26–34. https://doi.org/10.1016/j.apenergy.2015.08.031
84. Alam M, Kumar K, Verma S, Dutta V (2020) Renewable sources based DC microgrid using hydrogen energy storage: modelling and experimental analysis. Sustain Energy Technol Assess 42:100840. https://doi.org/10.1016/j.seta.2020.100840
85. Malheiro A, Castro PM, Lima RM, Estanqueiro A (2015) Integrated sizing and scheduling of wind/PV/diesel/battery isolated systems. Renew Energy 83:646–657. https://doi.org/10.1016/j.renene.2015.04.066
86. Ramli MA, Bouchekara H, Alghamdi AS (2018) Optimal sizing of PV/wind/diesel hybrid microgrid system using multi-objective self-adaptive differential evolution algorithm. Renew Energy 121:400–411. https://doi.org/10.1016/j.renene.2018.01.058
87. Maleki A, Ameri M, Keynia F (2015) Scrutiny of multifarious particle swarm optimization for finding the optimal size of a PV/wind/battery hybrid system. Renew Energy 80:552–563. https://doi.org/10.1016/j.renene.2015.02.045
88. Gan LK, Shek JK, Mueller MA (2015) Hybrid wind–photovoltaic–diesel–battery system sizing tool development using empirical approach, life-cycle cost and performance analysis: a case study in Scotland. Energy Convers Manage 106:479–494. https://doi.org/10.1016/j.enconman.2015.09.029
89. Liu Z, Chen Y, Zhuo R, Jia H (2018) Energy storage capacity optimization for autonomy microgrid considering CHP and EV scheduling. Appl Energy 210:1113–1125. https://doi.org/10.1016/j.apenergy.2017.07.002
90. Li S, Zhu G, Huang J, Tan Y, Chen C (2017) Analytical model of composite inertia control for wind turbine generators participating in frequency regulation. J Eng 2017(13):1164–1169. https://doi.org/10.1049/joe.2017.0512
91. Dakovic J, Ilak P, Baskarad T, Krpan M, Kuzle I (2018) Effectiveness of wind turbine fast frequency response control on electrically distanced active power disturbance mitigation. In: Mediterranean Conference on Power Generation, Transmission, Distribution and Energy Conversion (MEDPOWER2018). https://doi.org/10.1049/cp.2018.1923
92. Hu J, Sun L, Yuan X, Wang S, Chi Y (2017) Modeling of type 3 wind turbines with df/dt inertia control for system frequency response study. IEEE Trans Power Syst 32(4):2799–2809. https://doi.org/10.1109/TPWRS.2016.2615631
93. Xu H, Wang S, Hu J (2020) Mass–spring–damper modeling and stability analysis of type-4 wind turbines connected into asymmetrical weak AC grid. Energy Rep 6:649–655. https://doi.org/10.1016/j.egyr.2020.11.161
94. Belfkira R, Zhang L, Barakat G (2011) Optimal sizing study of hybrid wind/PV/diesel power generation unit. Sol Energy 85(1):100–110. https://doi.org/10.1016/j.solener.2010.10.018
95. Bilal BO, Sambou V, Ndiaye P, Kébé C, Ndongo M (2013) Multi-objective design of PV-wind-batteries hybrid systems by minimizing the annualized cost system and the loss of power supply probability (LPSP). In 2013 IEEE International Conference on Industrial Technology (ICIT); 861–868. https://doi.org/10.1109/ICIT.2013.6505784
96. Ma T, Yang H, Lu L (2014) A feasibility study of a stand-alone hybrid solar–wind–battery system for a remote island. Appl Energy 121:149–158. https://doi.org/10.1016/j.apenergy.2014.01.090
97. Rahimzadeh A, Christiaanse TV, Evins R (2021) Optimal storage systems for residential energy systems in British Columbia. Sustain Energy Technol Assess 45:101108. https://doi.org/10.1016/j.seta.2021.101108
98. Yang L, Hu Z, Xie S, Kong S, Lin W (2019) Adjustable virtual inertia control of supercapacitors in PV-based AC microgrid cluster. Electric Power Syst Res 173:71–85. https://doi.org/10.1016/j.epsr.2019.04.011
99. Zhang L et al (2021) Hybrid electrochemical energy storage systems: An overview for smart grid and electrified vehicle applications. Renew Sustain Energy Rev 139:110581. https://doi.org/10.1016/j.rser.2020.110581
100. Yang B et al (2020) Optimal sizing and placement of energy storage system in power grids: a state-of-the-art one-stop handbook. J Energy Storage 32:101814. https://doi.org/10.1016/j.est.2020.101814
101. Barelli L, Bidini G, Ciupageanu DA, Pelosi D (2021) Integrating hybrid energy storage system on a wind generator to enhance grid safety and stability: a levelized cost of electricity analysis. J Energy Storage 34:102050. https://doi.org/10.1016/j.est.2020.102050
102. de Siqueira LMS, Peng W (2021) Control strategy to smooth wind power output using battery energy storage system: a review. J Energy Storage 35:102252. https://doi.org/10.1016/j.est.2021.102252
103. Mahmoud M, Ramadan M, Olabi A-G, Pullen K, Naher S (2020) A review of mechanical energy storage systems combined with wind and solar applications. Energy Convers Manage 210:112670. https://doi.org/10.1016/j.enconman.2020.112670
104. Sedighizadeh M, Esmaili M, Mousavi-Taghiabadi SM (2019) Optimal joint energy and reserve scheduling considering frequency dynamics, compressed air energy storage, and wind turbines in an electrical power system. J Energy Storage 23:220–233. https://doi.org/10.1016/j.est.2019.03.019
105. Vidyanandan KV, Senroy N (2016) Frequency regulation in a wind–diesel powered microgrid using flywheels and fuel cells. IET Gener Transm Distrib 10(3):780–788. https://doi.org/10.1049/iet-gtd.2015.0449
106. Zargar MY, Mufti MU-D, Lone SA (2017) Adaptive predictive control of a small capacity SMES unit for improved frequency control of a wind-diesel power system. IET Renew Power Gener 11(14):1832–1840. https://doi.org/10.1049/iet-rpg.2017.0074
107. Zhu J et al (2018) Techno-economic analysis of MJ class high temperature Superconducting Magnetic Energy Storage (SMES) systems applied to renewable power grids. Global Energy Interconnect 1(2):172–178. https://doi.org/10.14171/j.2096-5117.gei.2018.02.009

108. Sheibani MR, Yousefi GR, Latify MA, Dolatabadi SH (2021) Energy storage system expansion planning in power systems: a review. IET Renew Power Gener 12(11):1203–1221. https://doi.org/10.1049/iet-rpg.2018.0089
109. Callec J, Caumon P, Capely L, Radvanyi E (2017) Benefits of large-scale energy storage systems in French islands. CIRED-Open Access Proc J 2017(1):1593–1596. https://doi.org/10.1049/oap-cired.2017.1110
110. Akram U, Nadarajah M, Shah R, Milano F (2020) A review on rapid responsive energy storage technologies for frequency regulation in modern power systems. Renew Sustain Energy Rev 120:109626. https://doi.org/10.1016/j.rser.2019.109626
111. Shayeghi H, Monfaredi F, Dejamkhooy A, Shafie-khah M, Catalão JPS (2021) Assessing hybrid supercapacitor-battery energy storage for active power management in a wind-diesel system. Int J Electr Power Energy Syst 125:106391. https://doi.org/10.1016/j.ijepes.2020.106391
112. Zhao T, Parisio A, Milanović JV (2021) Location-dependent distributed control of battery energy storage systems for fast frequency response. Int J Electr Power Energy Syst 125:106493. https://doi.org/10.1016/j.ijepes.2020.106493
113. Kadri A, Marzougui H, Aouiti A, Bacha F (2020) Energy management and control strategy for a DFIG wind turbine/fuel cell hybrid system with super capacitor storage system. Energy 192:116518. https://doi.org/10.1016/j.energy.2019.116518
114. Daraiseh F (2020) Frequency response of energy storage systems in grids with high level of wind power penetration—Gotland case study. IET Renew Power Gener 14(8):1282–1287. https://doi.org/10.1049/iet-rpg.2019.0628
115. Turk A, Sandelic M, Noto G, Pillai JR, Chaudhary SK (2019) Primary frequency regulation supported by battery storage systems in power system dominated by renewable energy sources. J Eng 2019(18):4986–4990. https://doi.org/10.1049/joe.2018.9349
116. Sebastián R (2016) Application of a battery energy storage for frequency regulation and peak shaving in a wind diesel power system. IET Gener Transm Distrib 10(3):764–770. https://doi.org/10.1049/iet-gtd.2015.0435
117. Wang L, Yu J-Y, Chen Y-T (2011) Dynamic stability improvement of an integrated offshore wind and marine-current farm using a flywheel energy-storage system. IET Renew Power Gener 5(5):387–396. https://doi.org/10.1049/iet-rpg.2010.0194
118. Farahani M, Ganjefar S (2013) Solving LFC problem in an interconnected power system using superconducting magnetic energy storage. Physica C 487:60–66. https://doi.org/10.1016/j.physc.2013.02.005
119. Jami M, Shafiee Q, Gholami M, Bevrani H (2020) Control of a super-capacitor energy storage system to mimic inertia and transient response improvement of a direct current micro-grid. J Energy Storage 32:101788. https://doi.org/10.1016/j.est.2020.101788
120. Abouzeid SI, Guo Y, Zhang H-C (2021) Cooperative control framework of the wind turbine generators and the compressed air energy storage system for efficient frequency regulation support. Int J Electr Power Energy Syst 130:106844. https://doi.org/10.1016/j.ijepes.2021.106844
121. Singh K (2021) Enhancement of frequency regulation in tidal turbine power plant using virtual inertia from capacitive energy storage system. J Energy Storage 35:102332. https://doi.org/10.1016/j.est.2021.102332
122. Magdy G, Mohamed EA, Shabib G, Elbaset AA, Mitani Y (2018) SMES based a new PID controller for frequency stability of a real hybrid power system considering high wind power penetration. IET Renew Power Gener 12(11):1304–1313. https://doi.org/10.1049/iet-rpg.2018.5096
123. Zarina PP, Mishra S, Sekhar PC (2012) Deriving inertial response from a non-inertial PV system for frequency regulation. In 2012 IEEE International Conference on Power Electronics, Drives and Energy Systems (PEDES) 2012;1–5. https://doi.org/10.1109/PEDES.2012.6484409
124. Alatrash H, Mensah A, Mark E, Haddad G, Enslin J (2012) Generator emulation controls for photovoltaic inverters. IEEE Trans Smart Grid 3(2):996–1011. https://doi.org/10.1109/TSG.2012.2188916
125. Liao S, Xu J, Sun Y, Bao Y, Tang B (2018) Wide-area measurement system-based online calculation method of PV systems de-loaded margin for frequency regulation in isolated power systems. IET Renew Power Gener 12(3):335–341. https://doi.org/10.1049/iet-rpg.2017.0272
126. Zarina PP, Mishra S, Sekhar PC (2014) Exploring frequency control capability of a PV system in a hybrid PV-rotating machine-without storage system. Int J Electr Power Energy Syst 60:258–267. https://doi.org/10.1016/j.ijepes.2014.02.033
127. Hoke AF, Shirazi M, Chakraborty S, Muljadi E, Maksimovic D (2017) Rapid active power control of photovoltaic systems for grid frequency support. IEEE J Emerging Select Top Power Electron 5(3):1154–1163. https://doi.org/10.1109/JESTPE.2017.2669299
128. Xin H, Liu Y, Wang Z, Gan D, Yang T (2013) A new frequency regulation strategy for photovoltaic systems without energy storage. IEEE Trans Sustain Energy 4(4):985–993. https://doi.org/10.1109/TSTE.2013.2261567
129. Watson LD, Kimball JW (2011) Frequency regulation of a microgrid using solar power. In: 2011 Twenty-sixth annual IEEE Applied power electronics conference and exposition (APEC). pp 321–326. https://doi.org/10.1109/APEC.2011.5744615
130. Ma HT, Chowdhury BH (2010) Working towards frequency regulation with wind plants: combined control approaches. IET Renew Power Gener 4(4):308–316. https://doi.org/10.1049/iet-rpg.2009.0100
131. Yao Q, Liu J, Hu Y (2019) Optimized active power dispatching strategy considering fatigue load of wind turbines during de-loading operation. IEEE Access 7:17439–17449. https://doi.org/10.1109/ACCESS.2019.2893957
132. Zhang X, Zha X, Yue S, Chen Y (2018) A frequency regulation strategy for wind power based on limited over-speed de-loading curve partitioning. IEEE Access 6:22938–22951. https://doi.org/10.1109/ACCESS.2018.2825363
133. Zhang J, Li Y, Xu Z, Qi D, Li C (2018) Game theory-based optimal deloading control of wind turbines under scalable structures of wind farm. IET Cyber-Phys Syst 3(4):224–231. https://doi.org/10.1049/iet-cps.2018.0027
134. Moutis P, Loukarakis E, Papathanasiou S, Hatziargyriou ND (2009) Primary load-frequency control from pitch-controlled wind turbines. In: 2009 IEEE Bucharest PowerTech; 1–7. https://doi.org/10.1109/PTC.2009.5281819
135. Moutis P, Papathanassiou SA, Hatziargyriou ND (2012) Improved load-frequency control contribution of variable speed variable pitch wind generators. Renew Energy 48:514–523. https://doi.org/10.1016/j.renene.2012.05.021
136. Žertek A, Verbič G, Pantoš M (2012) Optimised control approach for frequency-control contribution of variable speed wind turbines. IET Renew Power Gener 6(1):17–23. https://doi.org/10.1049/iet-rpg.2010.0233
137. Li M, Wang Y (2020) Research of frequency coordinated control strategy based on variable de-loading level for D-PMSG wind turbine. J Electr Eng Technol 15(6):2563–2576. https://doi.org/10.1007/s42835-020-00552-0
138. Vidyanandan KV, Senroy N (2013) Primary frequency regulation by deloaded wind turbines using variable droop. IEEE Trans Power Syst 28(2):837–846. https://doi.org/10.1109/TPWRS.2012.2208233

139. Abazari A, Dozein MG, Monsef H, Wu B (2019) Wind turbine participation in micro-grid frequency control through self-tuning, adaptive fuzzy droop in de-loaded area. IET Smart Grid 2(2):301–308. https://doi.org/10.1049/iet-stg.2018.0095
140. Zhu Z, Du S, Zhang L, Qi Q (2020) A new coordinated control strategy to improve the frequency stability of microgrid based on de-loaded capacity of wind turbine. In: 2020 5th Asia Conference on Power and Electrical Engineering (ACPEE); 645–651. https://doi.org/10.1109/ACPEE48638.2020.9136560
141. Singh K (2020) Load frequency regulation by de-loaded tidal turbine power plant units using fractional fuzzy based PID droop controller. Appl Soft Comput 92:106338. https://doi.org/10.1016/j.asoc.2020.106338
142. Liao S, Xu J, Sun Y, Bao Y, Tang B (2018) Wide-area measurement system-based online calculation method of PV systems de-loaded margin for frequency regulation in isolated power systems. IET Renew Power Generat 12(3):335–341. https://doi.org/10.1049/iet-rpg.2017.0272
143. Rafinia A, Moshtagh J, Rezaei N (2020) Towards an enhanced power system sustainability: An MILP under-frequency load shedding scheme considering demand response resources. Sustain Cities Soc 59:102168. https://doi.org/10.1016/j.scs.2020.102168
144. Sarasúa JI, Martínez-Lucas G, Pérez-Díaz JI, Fernández-Muñoz D (2021) Alternative operating modes to reduce the load shedding in the power system of El Hierro Island. Int J Electr Power Energy Syst 128:106755. https://doi.org/10.1016/j.ijepes.2020.106755
145. Singh AK, Fozdar M (2019) Event-driven frequency and voltage stability predictive assessment and unified load shedding. IET Gener Transm Distrib 13(19):4410–4420. https://doi.org/10.1049/iet-gtd.2018.6750
146. Huang B, Du Z, Liu Y, Zhao F (2017) Study on online under-frequency load shedding strategy with virtual inertia control of wind turbines. J Eng 2017(13):1819–1823. https://doi.org/10.1049/joe.2017.0645
147. Nascimento BDN, Souza ACZD, Costa JGDC, Castilla M (2019) Load shedding scheme with under-frequency and undervoltage corrective actions to supply high priority loads in islanded microgrids. IET Renew Power Generat 13(11):1981–1989. https://doi.org/10.1049/iet-rpg.2018.6229
148. Luo P, Wang X, Li Y (2020) The impact of datacenter load regulation on the stability of integrated power systems. Sustain Energy Technol Assess 42:100875. https://doi.org/10.1016/j.seta.2020.100875
149. Rafinia A, Rezaei N, Moshtagh J (2020) Optimal design of an adaptive under-frequency load shedding scheme in smart grids considering operational uncertainties. Int J Electr Power Energy Syst 121:106137. https://doi.org/10.1016/j.ijepes.2020.106137
150. Bhatti G, Mohan H, Singh RR (2021) Towards the future of smart electric vehicles: Digital twin technology. Renew Sustain Energy Rev 141:110801. https://doi.org/10.1016/j.rser.2021.110801
151. Humfrey H, Sun H, Jiang J (2019) Dynamic charging of electric vehicles integrating renewable energy: a multi-objective optimisation problem. IET Smart Grid 2(2):250–259. https://doi.org/10.1049/iet-stg.2018.0066
152. Ibrahim A, Jiang F (2021) The electric vehicle energy management: an overview of the energy system and related modeling and simulation. Renew Sustain Energy Rev 144:111049. https://doi.org/10.1016/j.rser.2021.111049
153. Joseph PK, Devaraj E, Gopal A (2019) Overview of wireless charging and vehicle-to-grid integration of electric vehicles using renewable energy for sustainable transportation. IET Power Electronics 12(4):627–638. https://doi.org/10.1049/iet-pel.2018.5127
154. Bibak B, Tekiner-Moğulkoç H (2021) A comprehensive analysis of Vehicle to Grid (V2G) systems and scholarly literature on the application of such systems. Renew Energy Focus 36:1–20. https://doi.org/10.1016/j.ref.2020.10.001
155. Sufyan M, Rahim NA, Muhammad MA, Tan CK, Raihan SRS, Bakar AHA (2020) Charge coordination and battery lifecycle analysis of electric vehicles with V2G implementation. Electric Power Syst Res 184:106307. https://doi.org/10.1016/j.epsr.2020.106307
156. Yao Y, Gao DW, Momoh J (2019) Dual-optimisation of power sources including plug-in electric vehicles and renewable energy resources at transmission-level system. J Eng 2019(5):3448–3454. https://doi.org/10.1049/joe.2018.5008
157. Liu H et al (2018) Enabling strategies of electric vehicles for under frequency load shedding. Appl Energy 228:843–851. https://doi.org/10.1016/j.apenergy.2018.06.122
158. Tavakoli A, Saha S, Arif MT, Haque ME, Mendis N, Oo AMT (2020) Impacts of grid integration of solar PV and electric vehicle on grid stability, power quality and energy economics: a review. IET Energy Syst Integr 2(3):243–260. https://doi.org/10.1049/iet-esi.2019.0047
159. Colmenar-Santos A, Muñoz-Gómez A-M, Rosales-Asensio E, López-Rey Á (2019) Electric vehicle charging strategy to support renewable energy sources in Europe 2050 low-carbon scenario. Energy 183:61–74. https://doi.org/10.1016/j.energy.2019.06.118
160. Liu H, Yang Y, Qi J, Li J, Wei H, Li P (2017) Frequency droop control with scheduled charging of electric vehicles. IET Gener Transm Distrib 11(3):649–656. https://doi.org/10.1049/iet-gtd.2016.0554
161. Wang X, He ZY, Yang JW (2019) Unified strategy for electric vehicles participate in voltage and frequency regulation with active power in city grid. IET Gener Transm Distrib 13(15):3281–3291. https://doi.org/10.1049/iet-gtd.2018.7016
162. Tang Y, Zhong J, Bollen M (2016) Aggregated optimal charging and vehicle-to-grid control for electric vehicles under large electric vehicle population. IET Gener Transm Distrib 10(8):2012–2018. https://doi.org/10.1049/iet-gtd.2015.0133
163. Deng R et al (2020) Exploring flexibility of electric vehicle aggregators as energy reserve. Electric Power Syst Res 184:106305. https://doi.org/10.1016/j.epsr.2020.106305
164. Gaur P, Bhowmik D, Soren N (2019) Utilisation of plug-in electric vehicles for frequency regulation of multi-area thermal interconnected power system. IET Energy Syst Integr 1(2):88–96. https://doi.org/10.1049/iet-esi.2018.0028
165. Muhssin MT, Obaid ZA, Al-Anbarri K, Cipcigan LM, Ajaweed MN (2021) Local dynamic frequency response using domestic electric vehicles. Int J Electr Power Energy Syst 130:106920. https://doi.org/10.1016/j.ijepes.2021.106920
166. Habib S, Kamran M, Rashid U (2015) Impact analysis of vehicle-to-grid technology and charging strategies of electric vehicles on distribution networks: a review. J Power Sources 277:205–214. https://doi.org/10.1016/j.jpowsour.2014.12.020
167. Nassar E, Tokimatsu K, Aziz M (2019) Potential distributions of electric vehicle secondary used batteries for frequency regulation in Europe. Energy Procedia 159:394–399. https://doi.org/10.1016/j.egypro.2018.12.070
168. Carrión M, Domínguez R, Cañas-Carretón M, Zárate-Miñano R (2019) Scheduling isolated power systems considering electric vehicles and primary frequency response. Energy 168:1192–1207. https://doi.org/10.1016/j.energy.2018.11.154
169. Chacko PJ, Sachidanandam M (2021) An optimized energy management system for vehicle to vehicle power transfer using micro grid charging station integrated Gridable Electric Vehicles. Sustain Energy Grids Netw 26:100474. https://doi.org/10.1016/j.segan.2021.100474

170. Magdy G, Ali H, Xu D (2021) A new synthetic inertia system based on electric vehicles to support the frequency stability of low-inertia modern power grids. J Clean Prod 297:126595. https://doi.org/10.1016/j.jclepro.2021.126595
171. Raveendran V, Alvarez-Bel C, Nair MG (2020) Assessing the ancillary service potential of electric vehicles to support renewable energy integration in touristic islands: a case study from Balearic island of Menorca. Renew Energy 161:495–509. https://doi.org/10.1016/j.renene.2020.06.083
172. Hwang M, Muljadi E, Park J-W, Sørensen P, Kang YCJITOSE (2016) Dynamic droop–based inertial control of a doubly-fed induction generator. IEEE Trans Sustain Energy 7(3):924–933. https://doi.org/10.1109/TSTE.2015.2508792
173. Gonzalez-Longatt F, Chikuni E, Rashayi E: Effects of the synthetic inertia from wind power on the total system inertia after a frequency disturbance. In: 2013 IEEE International Conference on Industrial Technology (ICIT); pp 826–832. https://doi.org/10.1109/ICIT.2013.6505779
174. Díaz-González F, Hau M, Sumper A, Gomis-Bellmunt OJR (2014) Participation of wind power plants in system frequency control: review of grid code requirements and control methods. Renew Sustain Energy Rev 34:551–564. https://doi.org/10.1016/j.rser.2014.03.040
175. Tarnowski GC, Kjar PC, Sorensen PE, Ostergaard J (2009) Variable speed wind turbines capability for temporary over-production. In: 2009 IEEE Power & Energy Society General Meeting; pp 1–7. https://doi.org/10.1109/PES.2009.5275387
176. Liu K, Qu Y, Kim H-M, Song HJITOPS (2017) Avoiding frequency second dip in power unreserved control during wind power rotational speed recovery. IEEE Trans Power Syst 33(3):3097–3106. https://doi.org/10.1109/TPWRS.2017.2761897
177. Morren J, De Haan SW, Kling WL, Ferreira JJITOPS (2006) Wind turbines emulating inertia and supporting primary frequency control. IEEE Trans Power Syst 21(1):433–434. https://doi.org/10.1109/TPWRS.2005.861956
178. Zhang W, Fang KJIG (2017) Controlling active power of wind farms to participate in load frequency control of power systems. IET Gener Transm Distrib 11(9):2194–2203. https://doi.org/10.1049/iet-gtd.2016.1471
179. Van de Vyver J, De Kooning JD, Meersman B, Vandevelde L, Vandoorn TL (2015) Droop control as an alternative inertial response strategy for the synthetic inertia on wind turbines. IEEE Trans Power Syst 31(2):1129–1138. https://doi.org/10.1109/TPWRS.2015.2417758
180. Su C, Chen Z (2012) Influence of wind plant ancillary frequency control on system small signal stability. In 2012 IEEE Power and Energy Society General Meeting; pp 1–8. https://doi.org/10.1109/PESGM.2012.6345411
181. Zhang Z, Wang Y, Li H, Su X (2013) Comparison of inertia control methods for DFIG-based wind turbines. In 2013 IEEE ECCE Asia Downunder; pp 960–964. https://doi.org/10.1109/ECCE-Asia.2013.6579222
182. Ray PK, Mohanty A (2019) A robust firefly–swarm hybrid optimization for frequency control in wind/PV/FC based microgrid. Appl Soft Comput 85:105823. https://doi.org/10.1016/j.asoc.2019.105823
183. Dhundhara S, Verma YP (2018) Capacitive energy storage with optimized controller for frequency regulation in realistic multisource deregulated power system. Energy 147:1108–1128. https://doi.org/10.1016/j.energy.2018.01.076
184. El-Fergany AA, El-Hameed MA (2017) Efficient frequency controllers for autonomous two-area hybrid microgrid system using social-spider optimiser. IET Gener Transm Distrib 11(3):637–648. https://doi.org/10.1049/iet-gtd.2016.0455
185. Jan MU, Xin A, Abdelbaky MA, Rehman HU, Iqbal S (2020) Adaptive and fuzzy PI controllers design for frequency regulation of isolated microgrid integrated with electric vehicle. IEEE Access 8:87621–87632. https://doi.org/10.1109/ACCESS.2020.2993178